Effect of mineral fillers on ageing of bituminous mastics

Mastoras, Filippos; Varveri, Aikaterini; van Tooren, Maaike; Erkens, Sandra

DOI
10.1016/j.conbuildmat.2020.122215

Publication date
2021

Document Version
Final published version

Published in
Construction and Building Materials

Construction and Building Materials 276 (2021) 122215

Contents lists available at ScienceDirect

Construction and Building Materials

journal homepage: www.elsevier.com/locate/conbuildmat

Effect of mineral fillers on ageing of bituminous mastics

Filippos Mastoras, Aikaterini Varveri *, Maaike van Tooren, Sandra Erkens

Delft University of Technology, Stevinweg 1, 2628CN Delft, the Netherlands

HIGHLIGHTS

- Filler particles increase the oxygen diffusion path in mastics, thus reducing bitumen oxidation.
- Active fillers lead to the increased formation of carbonyls in the bitumen matrix upon oxidative ageing.
- Basic fillers have a greater ability over acidic ones in adsorbing the polar functional groups from bitumen, preventing the viscosity build-up of mastics.

ARTICLE INFO

Article history:
Received 29 July 2020
Received in revised form 9 December 2020
Accepted 28 December 2020

Keywords:
Ageing
Bituminous mastics
Bitumen
Filler
Mineralogy

ABSTRACT

Past research has shown that the ageing process of bitumen is not solely a function of the bitumen type itself, but rather, added effects have been identified attributed to the presence of fillers. Nevertheless, contradicting results exist between the various studies with respect to the implications of fillers on the ageing process of bitumen. The present study aims to develop a better understanding regarding the role of the fillers in the ageing process of bitumen. Bitumen-filler blends (mastics) were prepared, according to a single design protocol, and the resulting materials along with pure bitumen were subjected to accelerated laboratory ageing by means of the pressure ageing vessel. The ageing effect was studied by using dynamic shear tests and infrared spectroscopy measurements. The results revealed the ability of fillers to mitigate age-hardening of bitumen, despite the fact that formation of carbonyls in the bitumen matrix was observed. Oxygen diffusion and adsorption mechanisms were found to be responsible for the observed favourable effect of fillers on the ageing of bitumen, while the gradation, the mineralogical/elemental composition and, to some extent, the specific surface area of the fillers where established as the prevailing fillers' properties regulating the oxidation mechanisms. The investigation of recovered binders from aged mastics did not lead to any further insight regarding the effect of fillers on the ageing of bitumen. Instead, features were revealed which manifest that the extraction and recovery of bitumen may not be a suitable approach to address the research question of this study.

1. Introduction

In practice, during the service life of an asphalt pavement, ageing occurs while bitumen is in contact with the mineral aggregates. Nevertheless, most ageing studies do not take into account the presence of minerals (aggregates, sand and filler) and their effect on the ageing process of bitumen. Instead, pure bitumen is subjected to ageing and further evaluated as an independent material [1]. This, provided that the mineral matter has indeed an effect on bitumen ageing, can lead to either underestimating or overestimating the ageing levels of bitumen due to the catalytic or mitigating effect of the mineral aggregates on bitumen ageing.

Amongst the two general aggregate fractions (i.e. coarse and fine) in an asphalt mixture, the fine fraction and its properties govern the physico-chemical interactions between the bitumen and the aggregates. In particular, the filler, which has substantially larger surface area than coarser fractions, provides the majority of the interfacial area where physico-chemical interactions between bitumen and aggregates occur [2]. Therefore, by conducting ageing studies on bitumen-filler systems, hereafter called mastics, any potential catalytic or mitigating effect of the mineral matter on the ageing of bitumen can be more readily captured and more clearly demonstrated. Moreover, in contrast to ageing studies on mixture level, factors that evidently affect the ageing process of bitumen and are of great variability among different studies, such as the air voids content in the asphalt mixture and the binder's film thickness that coats the aggregates, are eliminated since the filler can be viewed as being embedded in bitumen [3].

* Corresponding author.
E-mail address: a.varveri@tudelft.nl (A. Varveri).

https://doi.org/10.1016/j.conbuildmat.2020.122215
0950-0618/

Fillers may affect the ageing of bitumen through two main mechanisms. The first one is related to the physical presence of the filler particles in the mastic. The filler, being less permeable to air, compels the oxygen molecules to follow a spiral path in the diffusion medium, thus lengthening the diffusion path and reducing the rate of oxidative ageing of bitumen [4,5]. Moreover, the viscosity of bitumen increases upon addition of filler, which may lead to further hindrance of the oxygen diffusion process [4]. The second one is related to the interactions between bitumen and filler. On the one hand, the existence of certain mineral components on the filler surface may lead to the catalysis of bitumen oxidation [6]. On the other hand, an adsorption process may take place on the surface of the filler particles. In this case polar functional groups, that are naturally present in bitumen or are products of bitumen oxidation, are adsorbed and immobilized on the filler surface preventing the viscosity build-up of mastics [7,8].

Several studies are reported in literature investigating the effect of fillers on ageing of bitumen. Amongst them, the vast minority claims a catalysing effect of fillers on ageing of bitumen [9]. Most of them are aligned by demonstrating that fillers can mitigate bitumen ageing [1,3,7,10–12]. It is commonly recognized that the mineralogical and elemental composition as well as certain physical properties of the fillers (e.g. specific surface area and gradation) are major factors affecting the ageing process of bitumen. Nevertheless, contradicting results exist with respect to the effectiveness of different fillers with variable physico-chemical properties in decelerating bitumen ageing. In addition, a common line between relevant studies [3,11–13] is that the utilization of hydrated lime (either as base filler or as partial replacement of another base filler) enhances the mitigating action of the filler on ageing of bitumen. In the case, however, that hydrated lime is mixed with another base filler, its effectiveness can vary and is a function of its concentration and the type of the base filler used. The latter remarks highlight that a deeper understanding of the role of filler and the effect of its physico-chemical properties on the ageing process is yet to be achieved; this dictates the necessity for further fundamental research.

In this study, the effect of fillers on bitumen ageing is investigated by means of including fillers with distinct physico-chemical properties. The overall objective of this research is to provide fundamental insights on the role of different fillers in the ageing process of bitumen. A comparative analysis between the various bituminous mastics serves in establishing the mechanisms through which the effects of fillers on bitumen ageing occurs and identifying the governing filler properties that control these effects.

2. Materials and methods

2.1. Materials

2.1.1. Mineral fillers

Six different fillers were employed for the purpose of this study including both commercial and non-commercial materials. Wigro 60 K (WG60K) and Wigro (WG) are commercial fillers supplied by Sibelco Winterswijk and are composed of limestone with 25 wt% of hydrated lime (calcium hydroxide: $Ca(OH)_2$) and limestone (calcium carbonate: $CaCO_3$, category CC_{60}), respectively. WG60K is the specified filler currently used in the production of asphalt mixtures in the Netherlands, whose main purpose is to reduce the water sensitivity of asphalt mixtures [14], whereas WG was included in the study to represent basic aggregates. Also, baghouse dust (BD) (i.e. the dust generated during heating of the aggregates in the heating drum, which is collected and stored) was supplied by an asphalt plant operating in the region of the Netherlands. The utilization of the BD as filler in the production of asphalt mixtures could lead to the reduction of the overall production costs, hence it is of great interest to examine what are the implications of this by-product on bitumen ageing compared to the commercial fillers. Granite (GR) was considered in this study to represent acidic aggregates. The utilized GR originates from a Scottish quarry. Silverbond M6 or quartz (QZ) is a commercial filler supplied by Sibelco Dessel and is exclusively composed of quartz. It is hypothesized that, due to QZ's inert nature, no interactions will occur between this filler and the bitumen. Therefore, this filler was used to study its effects on the ageing of bitumen due to the physical presence of the filler particles in the mastic. Finally, Norwegian sandstone or bestone (BE) was included in the study for comparison reasons with the BD, since the utilized BD is most likely bestone according to the supplier's information.

Fig. 1 demonstrates the gradation curves of all fillers. A Sympatec HELOS laser diffraction instrument with a RODOS dry dispersion system combined with a VIBRI precise vibratory feeder was used for the derivation of the fillers' particles size distribution. WG60K and WG are the finest fillers followed by GR and BE, which show a rather similar gradation. BD and QZ are the coarser fillers, with the latter presenting the highest percentage of large particles.

Fig. 2 shows the environmental scanning electron microscope (ESEM) images of the fillers which were captured with a Philips XL30 ESEM-Tungsten filament electron microscope. The assessment of the surface characteristics of the fillers was done in a qualitative way (i.e. visually). WG60K and WG are mostly composed of granular type particles (red indicators) with very rough surface texture. BE and BD include both granular and angular type particles (green indicators). The BE particles show rougher surface texture than the BD particles. GR and QZ demonstrate the most angular particles with the latter being more pronounced in QZ. In addition, the QZ particles have the smoothest surface texture observed amongst all considered fillers. The ESEM images correlate well with fillers' gradations. The very fine nature of WG60K and WG and the coarseness of QZ are nicely captured in the microscope images, while the intermediate state, in terms of particles size distribution, of the rest of the fillers is also clearly shown in Fig. 2.

In Table 1 the properties of the fillers along with the applied methods are presented. The voids in the dry compacted fillers, or Rigden voids (RV), were determined by utilizing the Rigden equipment in accordance with NEN-EN 1097-4. The RV content is regulated by the particles' size, distribution, shape and surface texture [15]. The RV results can be correlated to the ESEM images of the fillers. WG60K shows the highest RV content amongst all fillers which is very well expected due to the presence of the granular

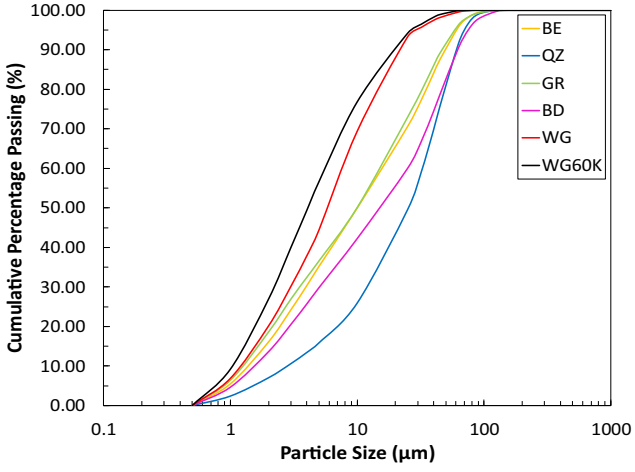

Fig. 1. Fillers gradation curves.

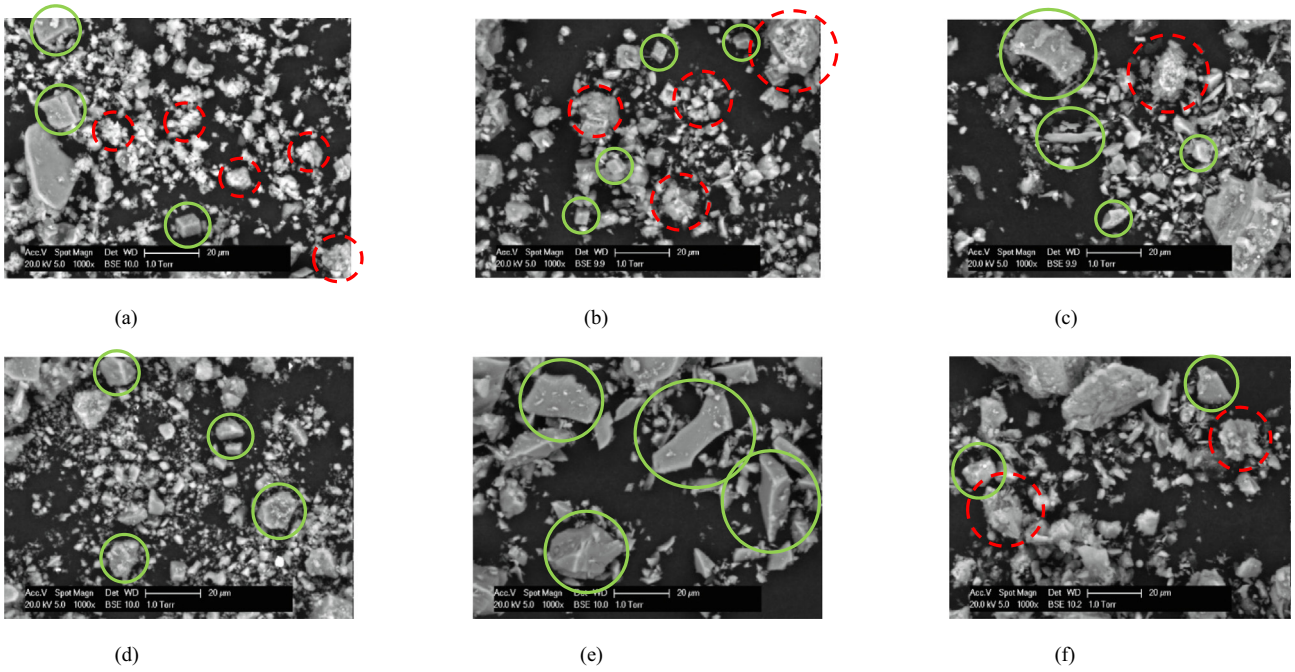

Fig. 2. ESEM images of (a) WG60K, (b) WG, (c) BD, (d) GR, (e) QZ, and (f) BE fillers.

Table 1
Fillers properties.

Property	Method	Units	Filler					
			WG60K	WG	BD	GR	QZ	BE
Density	NEN-EN 1097-7	gr/cm^3	2.54	2.77	2.68	2.64	2.64	2.70
Fineness Modulus	–	–	2.32	2.67	4.04	3.44	4.67	3.55
Rigden Voids	NEN-EN 1097-4	%	47.20	39.57	33.57	31.93	33.07	35.97
BET SSA	–	m^2/gr	8.51	13.25	2.61	3.03	0.80*	2.01
Methylene Blue	NEN-EN 933-9	gr/Kg	4.40	17.00	3.00	2.40	0.00	3.40

* Determined by sibelco dessel.

with rough surface texture hydrated lime particles (Fig. 2). When hydrated lime is added to another base filler the RV content increases with increasing amounts of hydrated lime. Typical values in the range of 45–50% are found for 25 wt% of hydrated lime in a filler mixture [16,17]. To cancel out the effect of the particles' size and size distribution it would be interesting to compare GR and BE, since their gradation is fairly similar. The morphological analysis of these fillers reveals that GR consists mostly of angular particles with intermediate surface roughness, whereas in BE mostly granular particles with rough surface are found. The latter observed differences, shape and texture-wise, are considered to entail a higher RV value for BE compared to GR Nevertheless, QZ presents a slightly higher RV value than GR, despite the fact that it evidently consists of exclusively angular type particles with the smoothest surface texture observed amongst the considered materials. This could be the result of the coarseness of QZ compared to GR in the context that the smaller particles of GR fill the voids between its larger particles, thus reducing the RV content.

The Braunauer-Emmett-Teller (BET) specific surface area (SSA) of the fillers was determined through nitrogen adsorption measurements using a dynamic vapor sorption (DVS) device. Fillers WG60K and WG possess the largest SSAs with the latter showing a very high value equal to 13.25 m^2/gr. The rest of the fillers show quite smaller values of SSA. Filler QZ has the smallest SSA which was measured equal to 0.80 m^2/gr.

The Methylene Blue (MB) test was conducted in accordance with NEN-EN 933-9 to determine harmful fines in the fillers, such as clay and organic materials. WG differentiates itself from the rest of the fillers by showing the highest MB value, which indicates a high illite content in comparison to the other filler samples (Table 3). WG is followed by WG60K, while BD and BE show quite similar MB values. Finally, GR has the lowest MB value amongst the fillers that seem to contain impurities, whereas QZ appears to be free of harmful fines by demonstrating no adsorption of the blue dye. The mineralogical analysis of fillers (Table 3) reveals that all materials, except QZ, contain clay minerals (i.e. mica and/or illite). WG demonstrates a relatively high concentration of mica and/or illite. Its high MB value denotes that this clay minerals group is governed by illite. On the contrary in the rest of the materials, which show substantially lower MB values, this group is governed by mica.

Table 2 shows the elemental composition of the fillers, as determined through X-Ray fluorescence spectroscopy (XRF) measurements, along with the results of the loss on ignition (LOI) test. The elemental analysis shows that the highest calcium compounds content appears in the limestone-based fillers (i.e. WG60K and WG). WG60K incorporates approximately 20% more calcium than WG, which is very well expected due to the added hydrated lime. QZ demonstrates a negligible calcium concentration, whereas SiO_2 is the governing element found in it. Overall, CaO and SiO_2 are the two elements in abundance in all fillers. Moreover, it is noticeable that the higher the CaO concentration the lower is the SiO_2 and vice versa. Fillers may be classified as acidic or basic based on their SiO_2 content [18] or, equivalently, based on their CaO content. Table 4 shows the basic-acidic classification of the utilized fillers.

Table 2
Fillers elemental composition.

Oxide	Chemical formula	Concentration (%)					
		WG60K	WG	BD	GR	QZ	BE
Iron	Fe_2O_3	1.193	2.377	3.015	1.958	0.034	3.711
Aluminium	Al_2O_3	2.933	5.526	9.242	14.485	0.150	11.533
Titanium	TiO_2	0.133	0.257	0.495	0.310	0.046	0.563
Potassium	K_2O	1.118	2.136	2.330	3.633	0.040	2.917
Calcium	CaO	49.510	30.240	16.457	2.015	0.026	8.657
Magnesium	MgO	3.950	9.430	1.953	0.720	0.008	2.266
Sodium	Na_2O	0.134	0.194	1.318	4.297	0.011	1.916
Silicon	SiO_2	9.960	16.570	51.880	70.719	99.571	60.716
Chromium	Cr_2O_3	–	–	0.014	0.012	0.001	0.016
Barium	BaO	0.009	0.021	0.076	0.127	0.004	0.087
Zirconium	ZrO_2	0.003	0.007	0.041	0.021	0.007	0.035
Strontium	SrO	0.044	0.147	0.042	0.046	–	0.049
LOI (%)		31.67*	33.21*	12.96**	1.34*	0.10*	7.24**

*Testing temperature: 1100 °C.
**Testing temperature: 950 °C.

Table 3
Fillers mineralogical composition.

Mineral	Concentration (%)					
	WG60K	WG	BD	GR	QZ	BE
Quartz	2.50	3.50	36.60	30.70	100.00	40.00
Plagioclase	–	–	12.10	40.20	–	17.80
K-Feldspar	2.50	6.30	6.70	21.00	–	7.20
Mica + Illite	7.00	12.80	12.10	2.10	–	15.80
Calcite	41.70	31.70	25.70	1.20	–	12.40
Chlorite	–	4.10	4.10	2.70	–	6.80
Pyroxene	–	–	–	2.10	–	–
Dolomite	17.30	41.30	2.10	–	–	–
Hematite	0.50	0.30	0.60	–	–	–
Portlandite	28.50	–	–	–	–	–

The X-Ray diffraction (XRD) test was used to reveal the mineralogical composition of the fillers and the results are summarized in Table 3. The governing minerals found in WG60K and WG are calcite and dolomite, which justifies their high calcium concentration (Table 2).

In addition, a high percentage of portlandite is found in WG60K, which is associated with the addition of hydrated lime. The latter is the reason why this mineral is only present in WG60K. Quartz is the only mineral found in QZ whereas this mineral is also present in a relatively high percentage (40%) in BE. BD shows the greatest diversity in minerals which seems as a reasonable result considering that BD is a by-product collected in the asphalt plant where different types of aggregates with distinct mineralogy may be used.

2.1.2. Bitumen and mastics

A single type of bitumen was used in this research, namely a 40/60 penetration grade bitumen. The conventional properties of the utilized binder are summarized in Table 5.

All mastics were prepared with a filler to bitumen mass ratio equal to 1 (f/b = 1.00 by mass) following the standard Dutch mix design. It should be noted that working with mass ratios might lead to different volumetric mix designs of the mastics for materials with very different densities. The detailed steps for the preparation of the materials are listed below.

Preparation of mastics:

- Bitumen and mineral filler were heated-up in the oven for 1 h at 130 °C.
- The appropriate amount of mineral filler, to achieve the intended filler to bitumen mass ratio (f/b = 1), was added to bitumen and the materials were manually stirred for 5 min. The applied stirring time ensured that a homogeneous blend was achieved while the workability of the mastic was kept at a tolerable level. The latter was enhanced by making use of a heating plate, set at 130 °C, during blending of the materials.
- The initial blending was followed by placing the mastic in the oven for 30 min at 130 °C. This step was added to enhance the bonding of the materials through application of heat.
- The mastic was manually re-stirred for 1 min to regain any mineral filler particles that might had migrated towards the bottom of the can and could affect the homogeneity of the mixture.
- "Fresh" mastic samples were obtained for the imminent tests while portion of the mastic was stored for the ageing procedure.

The abbreviations of the prepared mastics are shown in Table 6.

Preparation of reference bitumen:

- Bitumen was heated-up in the oven for 1 h at 130 °C.
- After the initial heating-up, bitumen was manually alligated for 5 min on a heating plate set at 130 °C.
- The material was placed in the oven for another 30 min at 130 °C, to match the age-hardening of the mastics.
- The bitumen was manually alligated for 1 min.
- "Fresh" samples were obtained for further testing, while a portion of the bitumen was stored for the ageing process.

The preparation of the mastics and neat bitumen, as described above, was followed by pouring an appropriate amount of the materials in the Pressure ageing vessel (PAV) pans for the imminent ageing test. Due to the high viscosity of the mastics, it was

Table 4
Fillers classification as basic or acidic.

Filler	Classification
WG60K	Basic
WG	
BD	
BE	
GR	
QZ	Acidic

Table 5
Pen 40/60 conventional properties.

Property	Method	Units	Pen 40/60
Penetration @ 25 °C	NEN-EN 1426	dmm	50.3
Softening point	NEN-EN 1427	°C	48.4
Density	–	gr/cm^3	1.03

not possible to achieve a uniform spread of the materials in the PAV pan by simply pouring the necessary amount. For that reason, the mastics in the PAV pans were placed in the oven for 15 min at 130 °C to allow for a decrease in their viscosity, which led to a uniform distribution of the materials in the metal trays. To preserve an equal ageing level between all materials, this added step was also applied on the referecnce bitumen, even though its viscosity was low enough, in the first place, to allow for its uniform spread in the PAV pan.

2.2. Methods

2.2.1. Pressure ageing vessel

The pressure ageing vessel (PAV) test was used to simulate the long-term ageing (LTA) of bitumen and mastics. The test was carried out in accordance with NEN-EN 14769, however, without prior short-term ageing (STA) of the materials by making use of the thin film oven test (TFOT) or the rolling thin film oven test (RTFOT). Past experience has shown that ageing of mastics in the TFOT may lead to the settlement of the filler particles at the bottom of the metal tray [7] due to the relatively high utilized temperature of ~163 °C [19]. Moreover, the RTFOT is an ageing test where the tested material forms a rotating film during ageing whose thickness is very much dependent on the material's viscosity. As a consequence, when mastic is tested with the RTFOT it is expected that its exposure to the hot air will be substantially less compared to bitumen, because of the different formed film thicknesses, which, in-turn, are controlled by the different viscosities of the materials. In a subsequent comparison of mastic and bitumen, the former would appear to be less aged, which could be incorrectly interpreted as a mitigating effect of the filler on ageing of bitumen [20]. Under the same considerations, uncertainty for the obtained outcome may also exist when mastics, incorporating different types of fillers, are tested with the RTFOT and then are evaluated for age-hardening in comparison with each other. In this case, a potential different stiffening effect of the various fillers could be the main reason behind observed differences. For the aforementioned reasons the STA of bitumen and mastics, as described in the NEN-EN 14769 standard, was omitted, since the reliability of the obtained results could be jeopardized.

The PAV test was conducted at a temperature of 90 °C and air pressure of 2.1 MPa (305 psi) for a duration of 20 h. The film thickness of the various mastics and bitumen during ageing in the PAV was kept constant and equal to 0.32 cm.

The completion of the accelerated ageing method was followed by placing the aged materials in the oven at 170 °C for 30 min, as suggested in NEN-EN 14769. This step is performed so that the aged material becomes fluid enough to allow for the removal of bubbles through manual stirring. The aged materials were manually stirred for 2 min, on a heating plate set at 170 °C, and aged samples were obtained for further testing.

2.2.2. Dynamic shear rheometer

The rheological evaluation of bitumen and mastics was done by utilizing an Anton Paar MCR 502 dynamic shear rheometer (DSR). Prior to the isothermal frequency sweep measurements, amplitude (i.e. stress) sweep tests were carried out on all mastics and bitumen, both at fresh and aged state, to determine their linear visco-elastic (LVE) region. The test was conducted at temperatures from −10 °C to 40 °C with 10 °C increments and a single frequency equal to 1 Hz. The LVE limit was defined as the point in the stress amplitude axis at which the maximum measured comple shear modulus value is reduced by 5% [21]. The results of the stress sweeps for the bitumen and the mastics are given in Appendix A.

By the outcome of the amplitude sweep measurements appropriate stress levels were chosen for each test temperature which fulfilled the condition that all materials were examined within their LVE region. Table 7 shows the selected stress levels, applied in the frequency sweep tests, per type of material and testing temperature.

The fundamental rheological properties, complex shear modulus (G^*) and phase angle (δ), of bitumen and mastics at different temperatures and frequencies were obtained by performing frequency sweep tests. Three replicates were tested for each material and their average was used to obtain the G^* and δ isothermal plots to be post- processed for the generation of master-curves. Table 8 summarizes the frequency sweep tests conditions.

G^* and δ master-curves were constructed at a reference temperature of 20 °C by implementing the time–temperature superposition principle. The necessary amount of shifting for each temperature (i.e. shift factors α_T) was calculated based on the Williams-Landel-Ferry (WLF) equation (Eq. (1)). The modified Christensen, Anderson and Marasteanu (CAM) model [22] was employed to describe the resulting G^* master-curves (Eq. (2)). The same mathematical expression was used to fit a smooth curve in the δ master-curves (Eq. (3)). The WLF constants, WLF shift factors and CAM model's fitting parameters for all tested materials are presented in Appendix B.

$$\log(\alpha_T) = -\frac{C_1 \cdot (T - T_{ref})}{C_2 + T - T_{ref}} \quad (1)$$

where α_T is the shift factor, T is the analyzed temperature (°C), T_{ref} is the reference temperature and C_1, C_2 are coefficients.

$$G^*(f) = G^*_e + \frac{G^*_g - G^*_e}{\left[1 + \left(\frac{f_c}{f}\right)^k\right]^{\frac{m}{k}}} \quad (2)$$

$$\delta(f) = \delta_e + \frac{\delta_g - \delta_e}{\left[1 + \left(\frac{f_d}{f}\right)^k\right]^{\frac{m}{k}}} \quad (3)$$

where $G^*(f)$ is the complex shear modulus as a function of the reduced frequency, f is the reduced frequency, G^*_e is the complex shear modulus at equilibrium state ($f \to 0$), G^*_g is the glassy complex shear modulus ($f \to -\infty$), f_c is a location parameter, k and m are shape parameters, $\delta(f)$ is the phase angle as a function of reduced frequency, δ_e is the phase angle at equilibrium state ($f \to 0$), δ_g is the phase angle when $f \to -\infty$ and f_d is a location parameter.

Table 6
Mastics abbreviations.

Mastic	Abbreviation
Pen 40/60 + Wigro 60 K	40/60_WG60K
Pen 40/60 + Wigro	40/60_WG
Pen 40/60 + Baghouse Dust	40/60_BD
Pen 40/60 + Granite	40/60_GR
Pen 40/60 + Quartz	40/60_QZ
Pen 40/60 + Bestone	40/60_BE

Table 7
Stress levels applied in the frequency sweep tests.

Temperature (°C)	Chosen stress level (Pa)	
	Mastics	Bitumen
−10	150,000	12,000
0	100,000	10,000
10	50,000	8000
20	7000	5000
30	2500	3000
40	2000	2000

Table 8
Frequency sweep test conditions.

Feature	Material	
	Mastic	Bitumen
Loading mode	Stress-controlled	Stress-controlled
Testing points	16	16
Test frequencies (Hz)	From 0.02 to 20.00	From 0.02 to 20.00
Test temperatures (°C)	−10, 0, 10, 20, 30, 40	−10, 0, 10, 20, 30, 40
Test geometry	8 mm plate, 2 mm gap	From −10 to 20 °C: 8 mm plate, 2 mm gap 30 & 40 °C: 25 mm plate, 1 mm gap

2.2.3. Fourier transform infrared spectroscopy

The chemical evaluation of bitumen and mastics was performed by utilizing a Perkin-Elmer Spectrum 100 Fourier transform infrared(FTIR) spectrometer with a single-point attenuated total reflectance (ATR) add-in. The FTIR was used to examine the bitumen ageing levels from a chemical point of view based on the formation of the two main products formed upon bitumen oxidation, the carbonyls (C = O) and the sulfoxides (S = O). The considered wave numbers region was set from 600 to 4000 cm^{-1}. Background checks and sample scans were carried out with twenty individual scans and a resolution of 4 cm^{-1}. For reproducibility reasons, three replicates were tested for each sample.

The post-processing of the FTIR raw data consisted of the normalization of the obtained spectra and the calculation of the carbonyls index (CI) and the sulfoxides index (SI). The absorbance of the asymmetric stretching vibration of the aliphatic group, at wave number 2923 cm^{-1}, was used for the spectra normalization (Eq. (4)) [23]. The boundary-wave numbers for the carbonyls and sulfoxides groups are presented in Table 9. The CI and SI were calculated according to Eq. (5) and Eq. (6), respectively, by making use of an absolute baseline (i.e. the horizontal wave numbers axis) [23].

$$y_{normalized}(x) = \frac{y(x)}{y(2923cm^{-1})} \quad (4)$$

$$CI = \int_{1666}^{1746} y_{normalized}(x)dx \quad (5)$$

$$SI = \int_{924}^{1066} y_{normalized}(x)dx \quad (6)$$

where $y_{normalized}(x)$ is the normalized absorbance value at wave number $\times$, $y(x)$ is the original absorbance value at wave number $\times$ and $y(2923\ cm^{-1})$ is the original absorbance value at wave number 2923 cm^{-1}.

3. Results and discussion

3.1. Mastic level

3.1.1. Rheological evaluation of bitumen and mastics

Fig. 3 shows the G* master-curves of bitumen and mastics both at the fresh and the aged state. The stiffening effect of filler when added to bitumen is nicely captured in Fig. 3, where the master-curves corresponding to the mastics offset towards higher values of the G* compared to the bitumen curve. Moreover, the master-curves are slightly shifted towards higher frequencies, demonstrating the more elastic response of mastics over bitumen.

Table 9
Area integration boundary-wave numbers.

Functional group	Lower boundary (cm^{-1})	Upper boundary (cm^{-1})
Carbonyls	1666	1746
Sulfoxides	924	1066

The effect of oxidative ageing on the shape of the G* master-curves is clearly shown in Fig. 3. Ageing led to the reduced time-dependency of the materials in the considered frequency range, which is expressed through the rotation (reduced slope) of the aged materials' master-curves with respect to the master-curves corresponding to the fresh ones. This effect of ageing on the materials' mechanical properties was very well expected and is in full agreement with previous research [1,3,24]. In addition, it can be observed that the reduction of the time-dependency is more pronounced in the case of bitumen which is an indication that the mastics underwent less severe ageing than the neat binder, aged under identical conditions.

Fig. 4 shows the δ master-curves of bitumen and mastics at fresh and aged states. The less viscous response of the unaged mastics, compared to the fresh bitumen, is demonstrated by their lower δ values, throughout the whole range of the considered frequencies, as well as by the shifting of their master-curves towards slightly higher frequencies. At the aged state, it is noticeable that bitumen shows lower δ values than all mastics at the intermediate to low frequencies region. This indicates that bitumen underwent more severe ageing than all mastics, as it was also deduced from the G* master-curves. In addition, it highlights the greater ability of all examined mastics over bitumen to dissipate shear stress through a more viscous response after ageing. On the contrary, at the region of intermediate to high frequencies all mastics demonstrate lower δ values than the bitumen, implying a more elastic behavior. This outcome at higher frequencies can be attributed to the intrinsic stiff nature of mastics and the simultaneous effect of low temperature behaviour.

3.1.2. Complex shear modulus ageing indices

The quantitative evaluation of the materials' ageing level was performed through the derivation of ageing indices (AIs) based on the G* master-curves. The AIs were calculated according to Eq. (7).

$$AI_i = \frac{G^*_{i,Aged}}{G^*_{i,Unaged}} \quad (7)$$

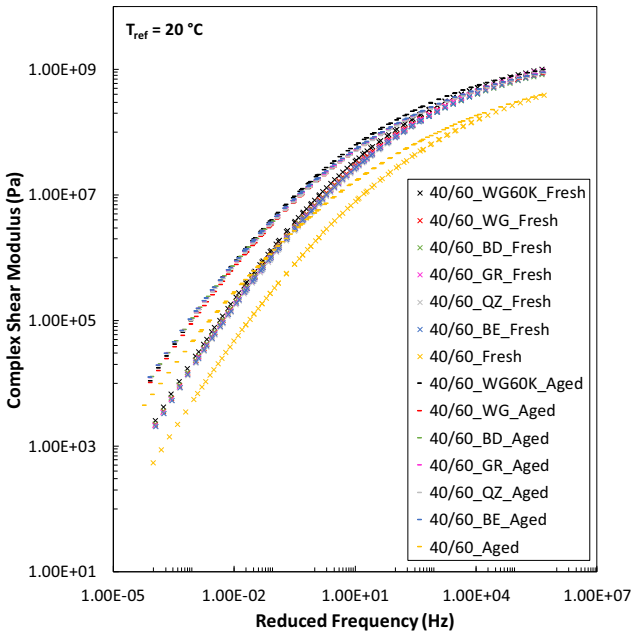

Fig. 3. Bitumen and mastics complex shear modulus master-curves at fresh and aged state.

where i is the reduced frequency at which the AI is evaluated, AI_i is the ageing index at reduced frequency i, $G^*_{i,\ Aged}$ is the complex shear modulus of the aged material at reduced frequency i and $G^*_{i,\ Unaged}$ is the complex shear modulus of the fresh material at reduced frequency i.

In Fig. 5 the calculated AIs of mastics and bitumen, as a function of reduced frequency, are presented. The effect of ageing is more pronounced at low frequencies (or at high temperatures), where the differences of the materials' ageing level become most apparent, while the AI curves converge to unit as the frequency increases. The latter is the result of the G* master-curves converging to the glassy modulus (G^*_g) at very high frequencies.

The results presented in Fig. 5 suggest that all fillers, regardless of their individual properties, have a mitigating effect on ageing of bitumen as it can be deduced by the mastics' lower G* AIs compared to bitumen throughout the whole range of the considered frequencies. The observed favourable effect of fillers on the ageing of bitumen is in full agreement with the results and conclusions reported elsewhere [1,3,7,8,10,11]. Mastics 40/60_WG60K and 40/60_WG show the least ageing amongst the tested materials and evidently their performance is quite comparable by virtue of the very close packing of their AI curves. The 40/60_BD mastic shows more severe ageing than the two limestone-based mastics which implies that the utilization of the dust collected in the asphalt plant as filler in the production of asphalt mixtures may lead to the deceleration of bitumen ageing, but its effect is still poorer than the one of the standardized filler currently used in the production of porous asphalt mixtures in the Netherlands (i.e. WG60K). The 40/60_GR and 40/60_QZ mastics also demonstrate quite similar results. However, a comparison of these two materials is not considered valid because, in contrast to GR, the inert QZ is not expected to develop interactions with bitumen and as a result the resulting ageing level of mastic 40/60_QZ is controlled by a single mechanism, solely related to the physical presence of the filler in the mastic. Finally, mastic 40/60_BE is the most aged mastic of all. It is noticeable that 40/60_BE mastic is even more aged than the 40/60_QZ mastic, prepared with the inert QZ. This outcome suggests that perhaps BE behaved as an inert filler, similarly to QZ, and no (favourable) interactions with bitumen occurred that would lead to a further reduction of the 40/60_BE mastic's ageing level, as in the case of the rest of the fillers.

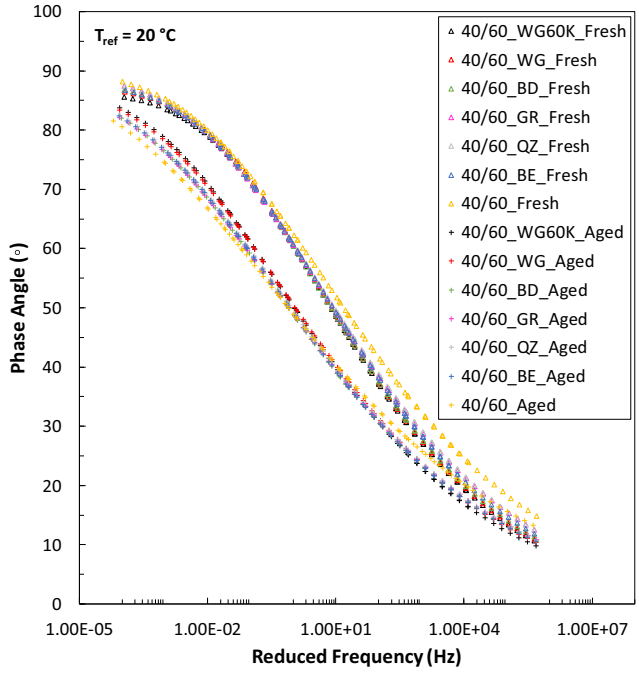

Fig. 4. Bitumen and mastics phase angle master-curves at fresh and aged state.

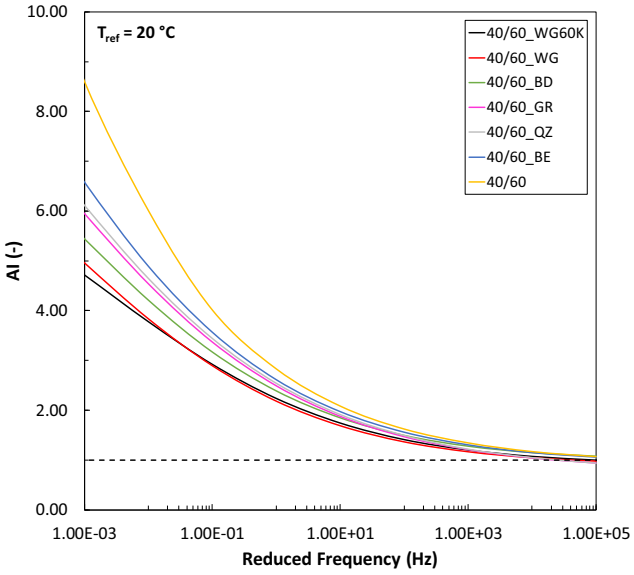

Fig. 5. Complex shear modulus ageing indices as a function of the reduced frequency at 20 °C.

3.1.3. Complex shear modulus ageing indices and fillers' properties correlation

Fig. 6 shows the G* AIs of all materials at 0.001 Hz and 20 °C, which was used for the comparison of the materials' ageing level in terms of figures and the correlation of the rheological results with the fillers' properties.

The 40/60_QZ mastic shows a lower G* AI than bitumen. This allows for the identification of the first mechanism through which the fillers' particles have a retarding effect on oxygen diffusion during ageing of the mastics. The relatively large difference between the AIs of mastic 40/60_QZ and bitumen can be attributed to the coarseness of QZ on the basis that the coarser the filler's particles the longer the path that the oxygen molecules follow when diffusing into the mastic. As mentioned previously, BE most likely behaved as an inert filler. So, having excluded the interactions with bitumen the remaining anti-ageing mechanism that characterizes BE is the effect of its particles on the oxygen diffusion path. BE is a finer filler than QZ which, based on the above analysis, can justify why mastic 40/60_BE has a higher AI than mastic 40/60_QZ.

Nevertheless, the fact that substantially finer fillers than QZ (e.g. WG60K and WG) led to less aged mastics than the 40/60_QZ mastic reveals that there exists another anti-ageing mechanism related to the interactions between filler and bitumen, which is responsible for the resulting ageing level of the materials. In addition, this observation suggests that the effect of filler particles on the oxygen diffusion path is a mechanism of secondary importance, whereas the developed interactions between the two mastic phases (i.e. filler and bitumen) seem to contribute the most to the mitigation of bitumen ageing.

The G* AIs presented in Fig. 6 show a good relationship with the fillers' ranking as basic or acidic. The basic limestone-based fillers WG60K and WG led to the least aged mastics while the acidic GR promoted the mitigation of bitumen ageing to a lesser extent. The BD lies in between the basic and acidic fillers which is in good agreement with its corresponding mastic ageing level (i.e. 40/60_BD). The inert QZ and the possibly inert-behaved BE led to the most aged mastics due to the lack of reactivity. A good relationship was established between the CaO concentration in fillers,

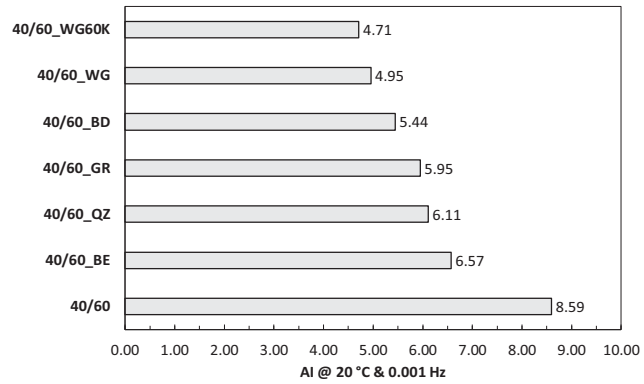

Fig. 6. Complex shear modulus ageing indices at 0.001 Hz and 20 °C.

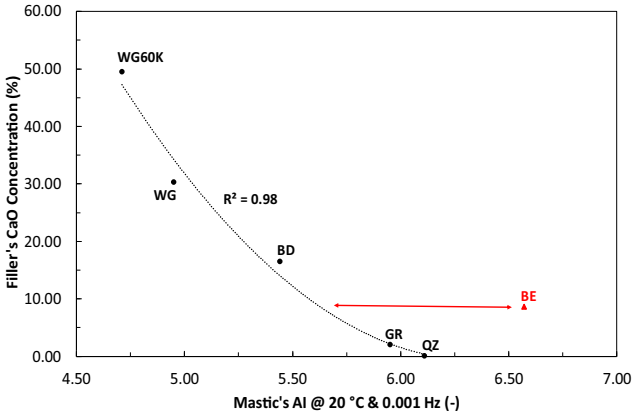

Fig. 7. Relationship between fillers' CaO concentration and mastics' complex shear modulus ageing indices at 0.001 Hz and 20 °C.

which is a relative measure of their basicity (or acidity), and the G* AIs of the mastics at 0.001 Hz and 20 °C as shown in Fig. 7. The results in Fig. 7 suggest that basic fillers possess a greater ability over the acidic ones to intensify the (favourable) interactions between the filler particles and the bitumen, thus leading to less aged mastics.

The SSA of the fillers is also believed to have an impact on the mitigation of bitumen ageing. A high SSA implies a large interface between the filler particles and the bitumen to interact [1]. Thus, it is quite reasonable to expect that when a filler presents a large SSA the interactions of the two materials are intensified. Fillers WG60K and WG possess the largest SSAs of all fillers, which can be another reason (besides their elemental/mineralogical composition, i.e. basic fillers) why mastics 40/60_WG60K and 40/60_WG demonstrate the least ageing (Fig. 6). Nevertheless, even though WG has a larger SSA than WG60K, the 40/60_WG mastic is still (slightly) more aged than the 40/60_WG60K mastic. This result suggests that the effect of the fillers' elemental/mineralogical composition may prevail over the effect of their SSA in mitigating the ageing of bitumen. This statement is further corroborated through a comparison of the BD and the GR. Despite the fact that the acidic GR has a larger SSA than the more basic BD, the 40/60_GR mastic is more aged than the 40/60_BD mastic, implying that the acidity of GR governs its behavior with respect to the mitigation of bitumen ageing. Finally, in Fig. 5 it is shown that the AI curves of mastics 40/60_WG60K and 40/60_WG are very closely packed, indicating a comparable effect of WG60K and WG on the ageing of bitumen. The close packing of the curves could be the result of the larger SSA of WG compared to WG60K, which compensates for their differences in the elemental/mineralogical composition. WG's larger SSA leads to a more pronounced intensification of the (favourable) interactions with bitumen. As a result, the AI curve of mastic 40/60_WG is brought close to the one of mastic 40/60_WG60K, prepared with the more basic filler WG60K.

3.1.4. Chemical evaluation of aged bitumen and mastics

Fig. 8 shows the close-up of the carbonyls' region. The chemical evaluation of the aged materials was performed through the calculation of the CI. The results of the CI are presented in Fig. 9.

The results show that the aged mastics prepared with the fillers WG60K, WG, BD and GR have higher CIs than the aged bitumen, which indicates the catalysis of bitumen oxidation in these mastics. The CI results in combination with the rheological evaluation of the ageing level of these materials verify the existence of an anti-ageing mechanism that is related to the interactions between the filler particles and the bitumen. This mechanism refers to the adsorption of polar bitumen components [1,7,8,10], apparently the ones formed upon oxidation, by the filler particles. More specifically, fillers WG60K, WG, BD and GR catalyzed the oxidation of bitumen, leading to higher concentration of carbonyls in their aged mastics compared to the aged bitumen. The G* AIs results (Figs. 5 and 6) are the outcome of the different abilities of fillers to adsorb and hold the polar functional groups from bitumen (e.g. carbonyls) on their particles' surface. As a result, the viscosity-build-up promoters are removed from the bitumen matrix, thus leading to apparent less aged mastics than the bitumen and entailing the mastics' relative ageing ranking.

Mastic 40/60_QZ_Aged shows a lower CI than the aged bitumen which implies that QZ did not lead to any catalysis of bitumen oxidation, as the aforementioned fillers did. This result may be attributed to the inertness of QZ. In addition, the aged mastic prepared with BE also shows a lower CI than the aged bitumen, similarly to mastic 40/60_QZ_Aged. This outcome suggests that perhaps BE indeed behaved as an inert filler.

3.2. Bitumen level

To assess the effect of fillers on the ageing of bituminous mixtures on bitumen level, binders were extracted and recovered from the aged mastics and subjected to DSR and FTIR testing. The solvent dichloromethane was utilized in the extraction phase. The recovery of bitumen from the bitumen-solvent solution was done

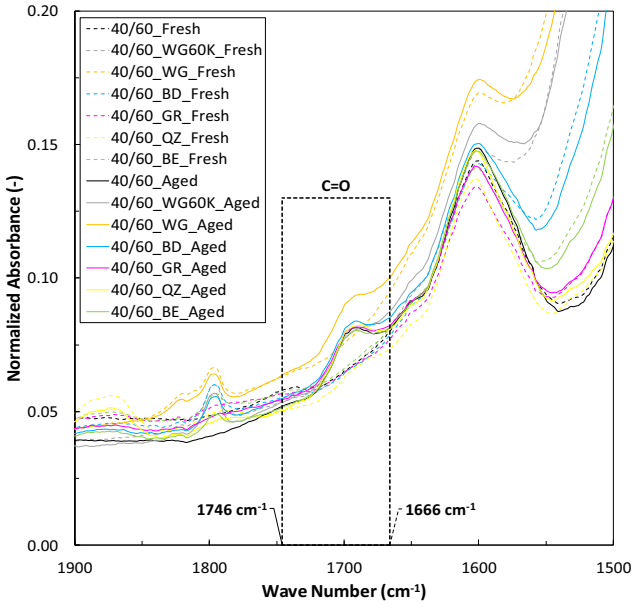

Fig. 8. Fresh and aged bitumen and mastics infrared spectra, carbonyls close-up.

according to NEN-EN 12697–3. Table 10 shows the abbreviations of the recovered binders.

3.2.1. Rheological evaluation of recovered binders

In Figs. 10 and 11 the G* and δ master-curves of the fresh, aged and recovered bitumen are presented, respectively, while Fig. 12 shows the G* AIs of the binders at 0.001 Hz and 20 °C as calculated based on Eq. (7).

All recovered binders appear to be less aged (or softer) than the neat aged bitumen based on the G* master-curves (Fig. 10) and the G* AIs (Fig. 12). This result is partially inconsistent with the mastics CIs results, presented in Fig. 9. In this figure it is showed that the aged mastics prepared with the fillers WG60K, WG, BD and GR show higher carbonyls concentration than the aged bitumen, whereas the rheological evaluation on bitumen level suggests that their recovered binders are less aged than the neat aged bitumen.

The irreversible adsorption of bitumen components (i.e. polar functional groups) on the filler particles could be a potential reason behind the observed softer behavior of the recovered binders compared to the neat aged bitumen [7]. Figs. 13 and 14 show the infrared spectra of the original and recovered fillers WG60K and WG, respectively. These two fillers are believed to experience the greatest adsorption of bitumen components. The results indicate that no new peaks appear in the infrared spectra of the recovered fillers that would denote the irreversible adsorption of bitumen components on the particles' surface, suggesting that all binders' components that might had reacted with the fillers were reclaimed back in the bitumen matrices upon extraction.

Two other possible reasons can be identified that might be responsible for the softer behavior of the recovered binders compared to the neat aged bitumen, which may operate individually or simultaneously. The first one is related to the reclamation of absorbed bitumen components upon extraction [7]. Oily and/or less polar components of bitumen might have been absorbed into the micropores of the filler particles upon the production of mastics. These components being protected (or much less affected) from volatilization and oxidation were reclaimed back into the bitumen matrices, imparting softening in the recovered binders. The second one refers to the solvent treatment of the aged mastics. Upon ageing the bitumen molecules form a dense molecular network. Dissolving in dichloromethane entails the almost complete destruction of this dense molecular network. Hence, the neat aged bitumen, which was not treated with solvent, still possesses this dense molecular network, making it stiffer than the recovered binders.

3.2.2. Chemical evaluation of recovered binders

In Fig. 15, the infrared spectra of all recovered binders as well as of the neat fresh and aged bitumen are presented. At the sulfoxides region (S = O) it can be observed that the spectrum of the RB_40/60_GR_Aged shows an unusually large peak. The disturbance of the shape of the infrared spectrum at this region is the

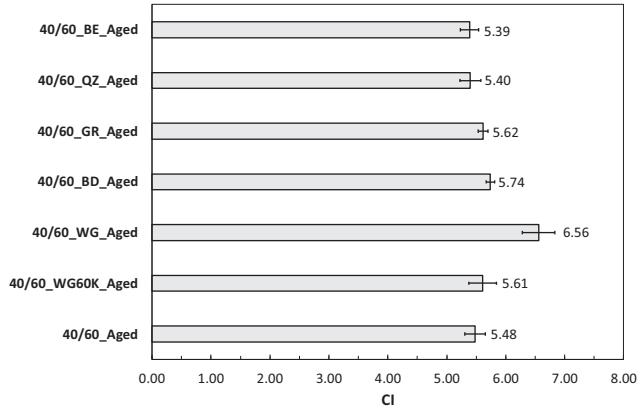

Fig. 9. Aged bitumen and mastics carbonyls indices.

Table 10
Recovered bitumen abbreviations.

Treated mastic	Recovered bitumen abbreviation
40/60_WG60K_Aged	RB_40/60_WG60K_Aged
40/60_WG_Aged	RB_40/60_WG_Aged
40/60_BD_Aged	RB_40/60_BD_Aged
40/60_GR_Aged	RB_40/60_GR_Aged
40/60_QZ_Aged	RB_40/60_QZ_Aged
40/60_BE_Aged	RB_40/60_BE_Aged

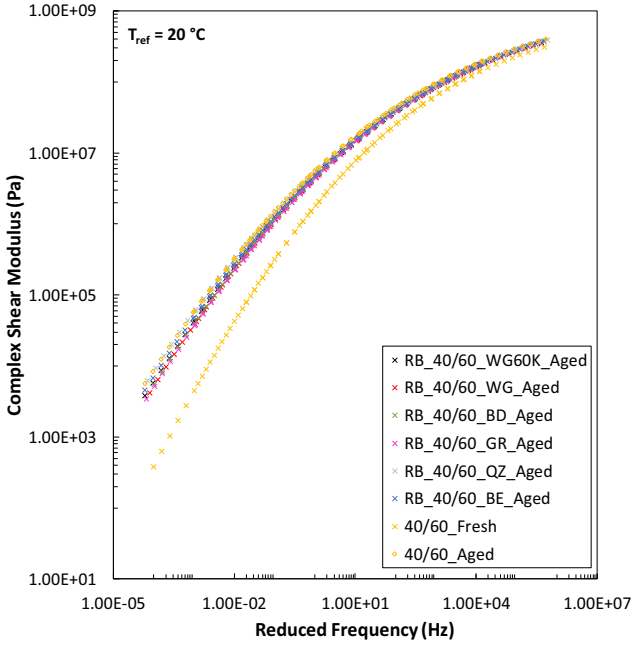

Fig. 10. Fresh, aged and recovered bitumen complex shear modulus master-curves.

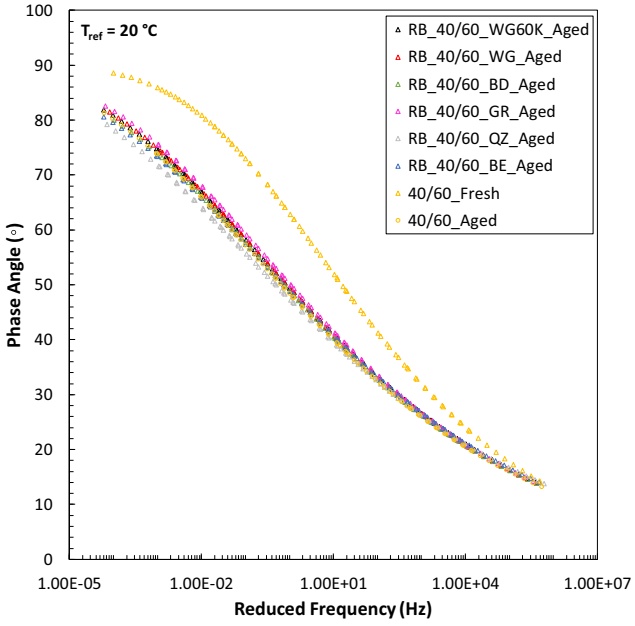

Fig. 11. Fresh, aged and recovered bitumen phase angle master-curves.

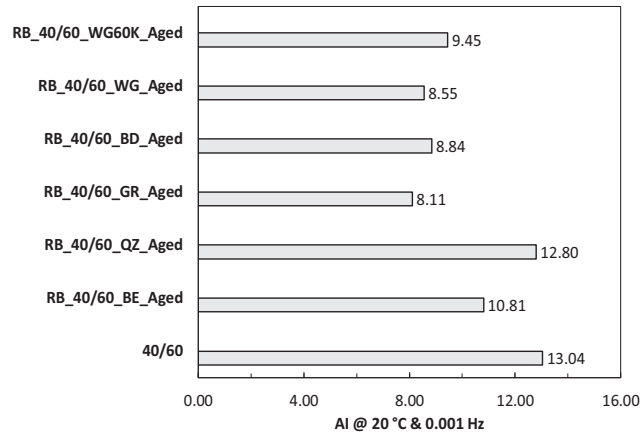

Fig. 12. Fresh, aged and recovered bitumen complex shear modulus ageing indices at 0.001 Hz and 20 °C.

result of filler residue in the recovered bitumen and can be ascribed to the peak of the infrared spectrum of filler GR around the wave number 1030 cm^{-1}. The latter is demonstrated in Fig. 16 (circled area), where the infrared spectrum of the neat aged bitumen is also depicted for comparison reasons. The disturbance at this region leads to an increased SI for the recovered bitumen from the GR aged mastic (Fig. 18).

The results in Figs. 17 and 18 demonstrate that more carbonyls and sulfoxides are formed in the recovered binders compared to the neat aged bitumen, indicating the more severe ageing of the former compared to the latter. This result is in complete contrast with the rheological evaluation of the recovered binders (Figs. 10 and 12) which appeared to be less aged than the neat aged bitumen. This contradiction between the DSR and FTIR results suggests that the previously mentioned reasons regarding the softening of the recovered binders might indeed hold true. Moreover, the CI and SI results verify that fillers WG60K, WG, BD and GR led to the catalysis of bitumen oxidation in their respective mastics. On the other hand, this effect is not captured in the rheological evaluation of the mastics, possibly due to the differences in the ability of the fillers to adsorb polar functional groups from the bitumen matrix, which lead to apparent less aged mastics than the neat bitumen.

The recovered binders from the BE and QZ aged mastics also show higher indices of carbonyls and sulfoxides than the neat aged bitumen, which does not agree with the rheological and chemical evaluation of the mastics. This outcome at bitumen level might be the result of the effect of the hot extraction and recovery process on the carbonyl and sulphoxide formation in the recovered binders.

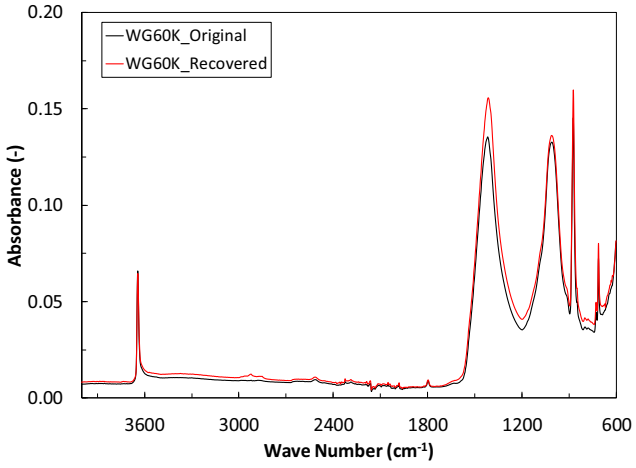

Fig. 13. Original and recovered filler WG60K infrared spectra.

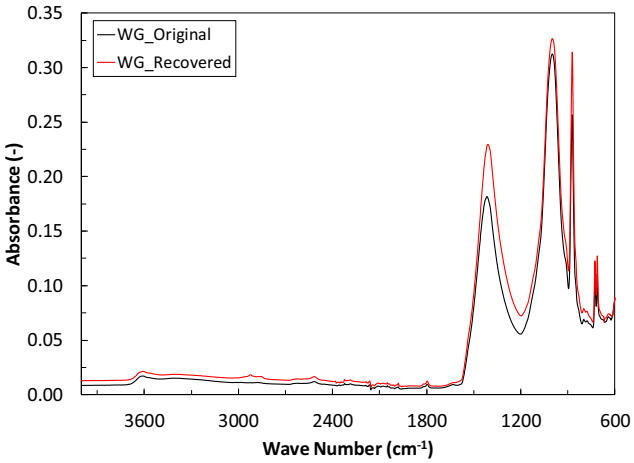

Fig. 14. Original and recovered filler WG infrared spectra.

4. Summary and Conclusions

In this study the effect of six different filler types on the ageing of bitumen was investigated. Neat bitumen and mastics, prepared with a filler to bitumen mass ratio equal to one, were aged in the PAV and their changes in rheology and chemistry were evaluated. In an effort to gain further insight into the effect of fillers on bitumen ageing, binders were extracted from the aged mastics and their rheological and chemical properties were determined.

The aged mastic prepared with the inert filler quartz shows a complex shear modulus ageing index (at 0.001 Hz and 20 °C) equal to 6.11 while the neat aged bitumen has an ageing index equal to 8.59. This outcome implies the existence of an anti-ageing mechanism related to the physical presence of the filler particles in the mastic and their retarding effect on the diffusion of oxygen. The aged mastic prepared with the active filler bestone has an ageing index equal to 6.57. This mastic is less aged than bitumen but more aged than the quartz mastic. This outcome suggests that most likely bestone filler did not develop any interactions with bitumen but, rather, behaved as an inert filler similarly to quartz. The more severe ageing of the bestone mastic compared to quartz mastic

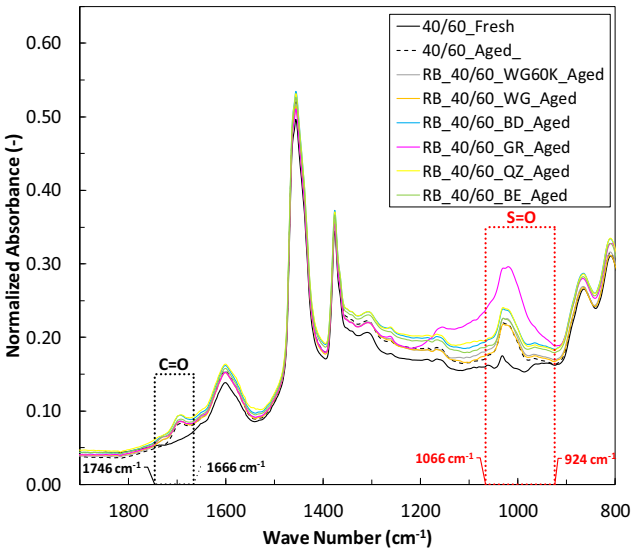

Fig. 15. Fresh, aged and recovered bitumen infrared spectra.

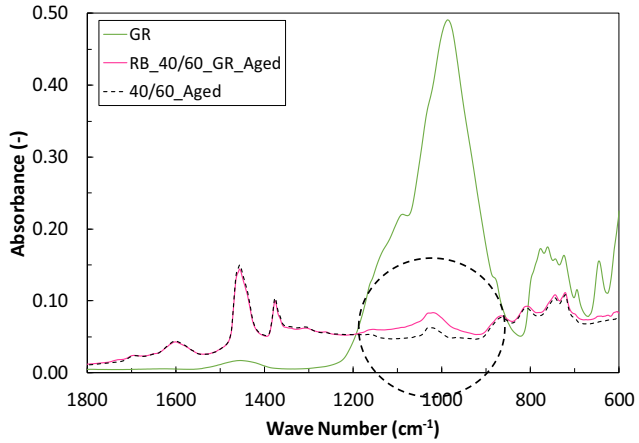

Fig. 16. Effect of GR filler residue on recovered binder's infrared spectrum.

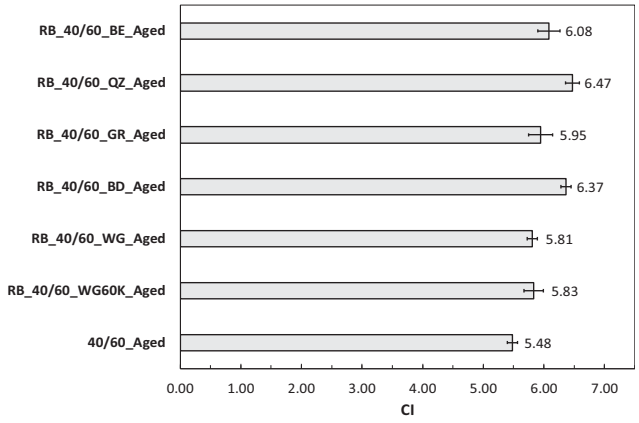

Fig. 17. Aged and recovered bitumen carbonyls indices.

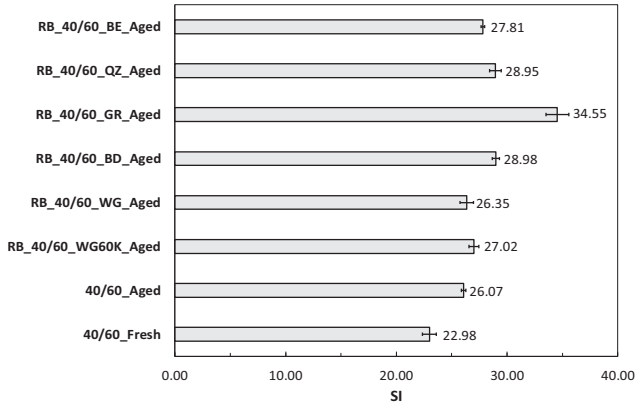

Fig. 18. Fresh, aged and recovered bitumen sulfoxides indices.

leads to the conclusion that coarser fillers have a more favourable effect on the ageing of bitumen, when only their physical presence in the mastic is considered.

The aged mastics prepared with the active fillers Wigro 60 K, Wigro, baghouse dust and granite show a complex shear modulus ageing index (at 0.001 Hz and 20 °C) equal to 4.71, 4.95, 5.44 and 5.95, respectively, demonstrating their less severe ageing compared to the neat aged bitumen and the quartz aged mastic. This result suggests the existence of a prevailing anti-ageing mechanism, which refers to the adsorption of bitumen polar functional groups on the filler particle surface, which are not allowed to contribute to the viscosity build-up of the mastics. The difference in the ageing indices of the various mastics prepared with the active fillers is the result of the different effectiveness of these fillers in adsorbing bitumen components. The established relationship between the filler CaO concentration and the mastic complex shear modulus ageing indices at 0.001 Hz and 20 °C indicates that the adsorption ability of fillers is controlled by their elemental/mineralogical composition. Basic fillers (i.e. high CaO concentration) possess a greater ability over more acidic ones (i.e. rich in SiO_2) in removing polar functional groups from the bitumen matrix.

Fillers Wigro 60 K and Wigro led to mastics that demonstrated a rather equivalent performance, ageing-wise, based on the complex shear modulus ageing indices curves. This observation leads to the conclusion that, the 25 wt% of hydrated lime present in Wigro 60 K does not result in an enhanced effectiveness of this filler, compared to Wigro (pure limestone) to mitigate the ageing of bitumen.

The aged mastics prepared with the active fillers Wigro 60 K, Wigro, baghouse dust and granite showed carbonyls indices of 5.61, 6.56, 5.74 and 5.62, respectively, all being higher that the carbonyl index of aged birumen which is equal to 5.48. This result indicates that the active fillers, in fact, facilitated the oxidation of bitumen and that the outcome of the rheological evaluation could be indeed attributed to an adsorption mechanism. On the other hand, the aged mastics prepared with the inert filler quartz and bestone have a carbonyls index equal to 5.40 and 5.39, respectively, showing less concentration of oxygenated products that the neat aged bitumen. In contrast to the active fillers, the inert fillers did not lead to any catalysis of bitumen ageing. Regarding bestone, the outcome of the FTIR analysis verifies that this filler behaved as an inert filler.

The extraction and recovery of bitumen from the aged mastics did not result in any further insight regarding the effect of fillers on the ageing of bitumen. Instead, the rheological evaluation at bitumen level revealed that the recovered binders do not reflect the actual state of the effective bitumen in the filler-bitumen systems. It is suggested that in future studies the reference bitumen undergoes the exact same solvent treatment as the recovered binders for a more fair comparison of the materials. The results of the chemical evaluation of the recovered binders showed a similar generic trend with the results obtained at mastic level. Nevertheless, it is believed that the carbonyl and sulfoxide indices at bitumen level include the effect of the hot extraction and recovery process on the properties of the recovered binders; hence the reliability of the indices is questionable.

CRediT authorship contribution statement

Filippos Mastoras: Methodology, Formal analysis, Investigation, Writing - review & editing. **Aikaterini Varveri:** Conceptualization, Methodology, Formal analysis, Investigation, Writing - review & editing, Supervision, Funding acquisition. **Maaike Tooren:** Methodology, Writing - review & editing. **Sandra Erkens:** Methodology, Resources, Funding acquisition.

Declaration of Competing Interest

The authors declare that they have no known competing financial interests or personal relationships that could have appeared to influence the work reported in this paper.

Acknowledgements

The authors gratefully acknowledge the contribution of Sibelco Winterswijk and Sibelco Dessel to the realization of this study. The contribution of Ing. Wim Verwaal (Delft University of Technology) to this work on the characterization of the filler properties is gratefully acknowledged.

Appendix A Stress sweep test results

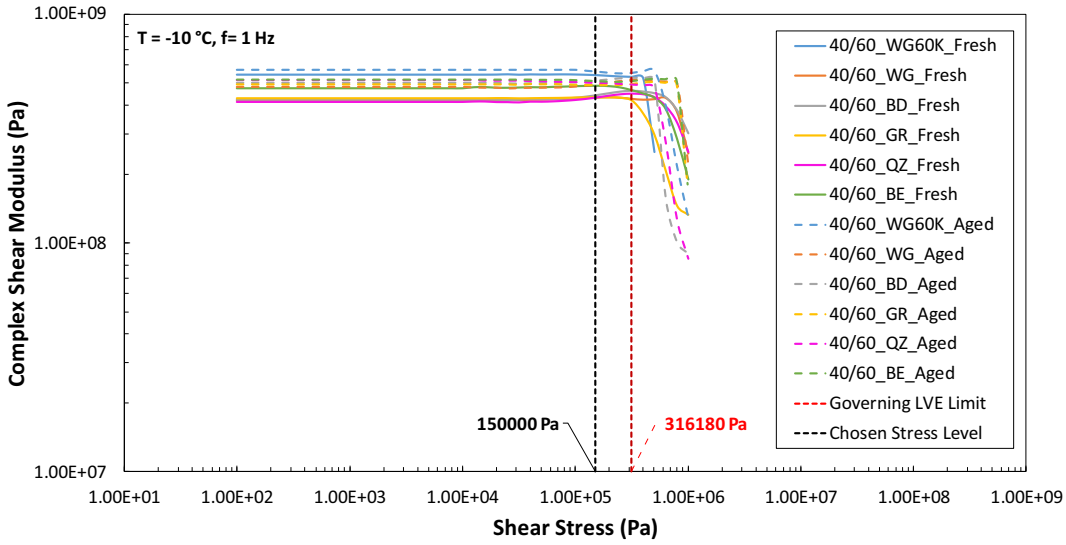

Fig. A1. Mastics amplitude sweep test results. T = −10 °C, f = 1 Hz.

Table A1
Mastics LVE limits. T = −10 °C, f = 1 Hz.

Mastic	G^*_{max} (Pa)	$0.95G^*_{max}$ (Pa)	τ_{limit} (Pa)	$\tau_{governing}$ (Pa)	τ_{chosen} (Pa)
40/60_WG60K_Fresh	546490000.0	519165500.0	398050.0	316180	150000
40/60_WG_Fresh	432040000.0	410438000.0	398050.0		
40/60_BD_Fresh	463620000.0	440439000.0	501000.0		
40/60_GR_Fresh	434680000.0	412946000.0	316180.0		
40/60_QZ_Fresh	448350000.0	425932500.0	500990.0		
40/60_BE_Fresh	486010000.0	461709500.0	316180.0		
40/60_WG60K_Aged	570820000.0	542279000.0	501010.0		
40/60_WG_Aged	515120000.0	489364000.0	794210.0		
40/60_BD_Aged	526600000.0	500270000.0	501010.0		
40/60_GR_Aged	505820000.0	480529000.0	794210.0		
40/60_QZ_Aged	517240000.0	491378000.0	316180.0		
40/60_BE_Aged	521440000.0	495368000.0	794210.0		

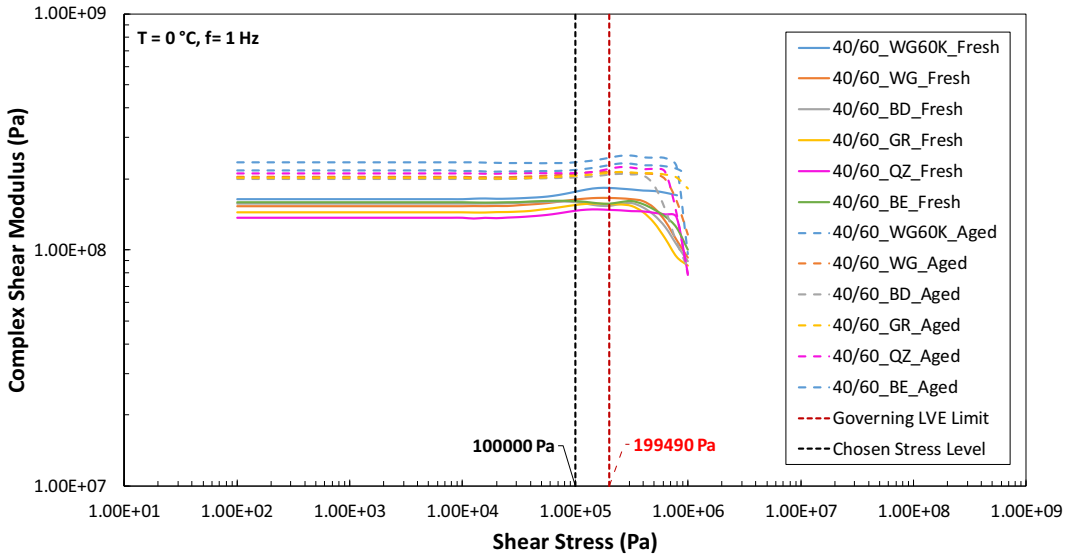

Fig. A2. Mastics amplitude sweep test results. T = 0 °C, f = 1 Hz.

Table A2
Mastics LVE limits. T = 0 °C, f = 1 Hz.

Mastic	G^*_{max} (Pa)	$0.95G^*_{max}$ (Pa)	τ_{limit} (Pa)	$\tau_{governing}$ (Pa)	τ_{chosen} (Pa)
40/60_WG60K_Fresh	183740000.0	174553000.0	630840.0	199490	100000
40/60_WG_Fresh	165730000.0	157443500.0	398030.0		
40/60_BD_Fresh	160900000.0	152855000.0	199490.0		
40/60_GR_Fresh	157280000.0	149416000.0	316170.0		
40/60_QZ_Fresh	148310000.0	140894500.0	630840.0		
40/60_BE_Fresh	161570000.0	153491500.0	398030.0		
40/60_WG60K_Aged	251730000.0	239143500.0	630850.0		
40/60_WG_Aged	213810000.0	203119500.0	501100.0		
40/60_BD_Aged	209480000.0	199006000.0	398030.0		
40/60_GR_Aged	214070000.0	203366500.0	794170.0		
40/60_QZ_Aged	225150000.0	213892500.0	630840.0		
40/60_BE_Aged	232490000.0	220865500.0	794180.0		

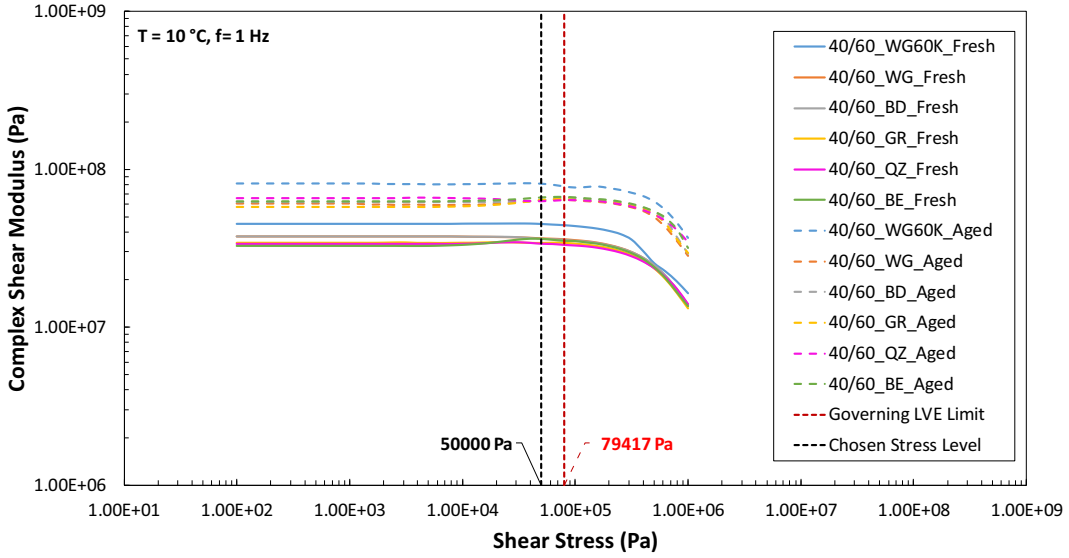

Fig. A3. Mastics amplitude sweep test results. T = 10 °C, f = 1 Hz.

Table A3
Mastics LVE limits. T = 10 °C, f = 1 Hz.

Mastic	G^*_{max} (Pa)	$0.95G^*_{max}$ (Pa)	τ_{limit} (Pa)	$\tau_{governing}$ (Pa)	τ_{chosen} (Pa)
40/60_WG60K_Fresh	45196000.0	42936200.0	99975.0	79417	50000
40/60_WG_Fresh	37646000.0	35763700.0	79419.0		
40/60_BD_Fresh	37430000.0	35558500.0	79417.0		
40/60_GR_Fresh	34523000.0	32796850.0	125870.0		
40/60_QZ_Fresh	34552000.0	32824400.0	99990.0		
40/60_BE_Fresh	36143000.0	34335850.0	99990.0		
40/60_WG60K_Aged	81445000.0	77372750.0	158460.0		
40/60_WG_Aged	63951000.0	60753450.0	199480.0		
40/60_BD_Aged	65973000.0	62674350.0	199480.0		
40/60_GR_Aged	64996000.0	61746200.0	199480.0		
40/60_QZ_Aged	66049000.0	62746550.0	158460.0		
40/60_BE_Aged	66838000.0	63496100.0	199480.0		

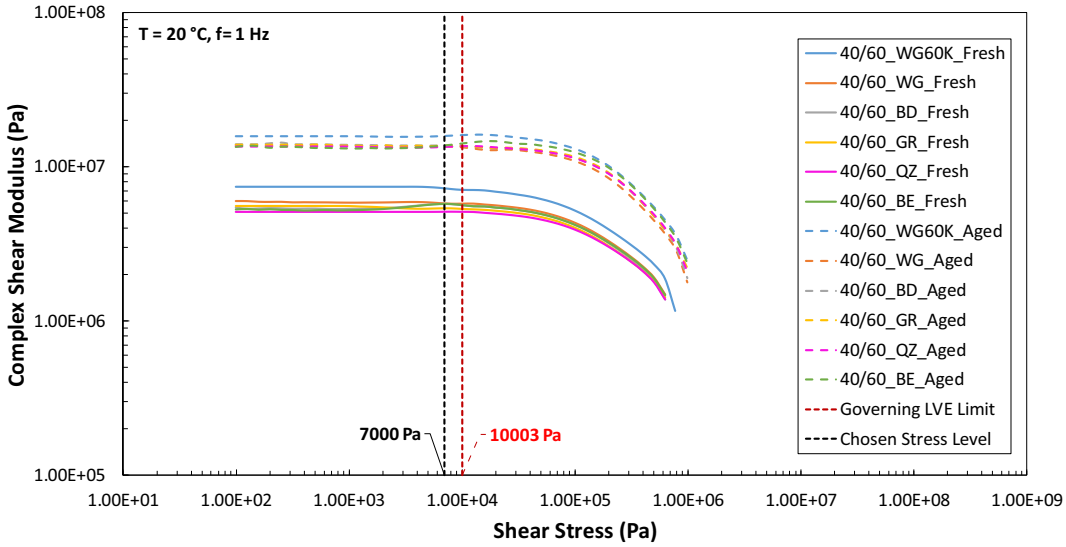

Fig. A4. Mastics amplitude sweep test results. T = 20 °C, f = 1 Hz.

Table A4
Mastics LVE limits. T = 20 °C, f = 1 Hz.

Mastic	G^*_{max} (Pa)	$0.95G^*_{max}$ (Pa)	τ_{limit} (Pa)	$\tau_{governing}$ (Pa)	τ_{chosen} (Pa)
40/60_WG60K_Fresh	7417600.0	7046720.0	12606.0	10003	7000
40/60_WG_Fresh	6020500.0	5719475.0	12610.0		
40/60_BD_Fresh	5750900.0	5463355.0	15875.0		
40/60_GR_Fresh	5609200.0	5328740.0	12611.0		
40/60_QZ_Fresh	5112700.0	4857065.0	25165.0		
40/60_BE_Fresh	5772500.0	5483875.0	15876.0		
40/60_WG60K_Aged	16260000.0	15447000.0	31628.0		
40/60_WG_Aged	13793000.0	13103350.0	12591.0		
40/60_BD_Aged	14360000.0	13642000.0	10003.0		
40/60_GR_Aged	14030000.0	13328500.0	31628.0		
40/60_QZ_Aged	13643000.0	12960850.0	31627.0		
40/60_BE_Aged	14750000.0	14012500.0	39819.0		

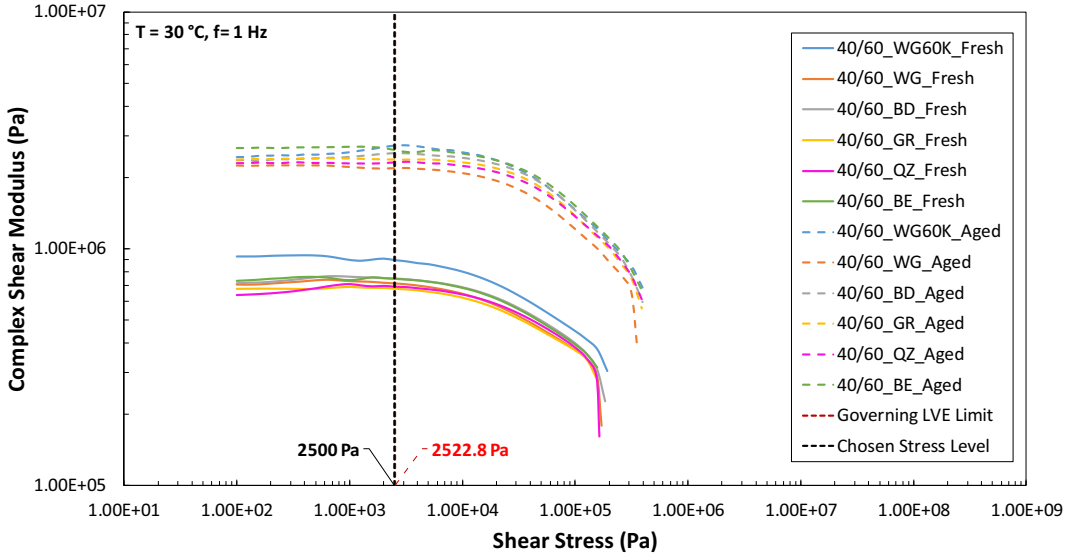

Fig. A5. Mastics amplitude sweep test results. T = 30 °C, f = 1 Hz.

Table A5
Mastics LVE limits. T = 30 °C, f = 1 Hz.

Mastic	G^*_{max} (Pa)	$0.95G^*_{max}$ (Pa)	τ_{limit} (Pa)	$\tau_{governing}$ (Pa)	τ_{chosen} (Pa)
40/60_WG60K_Fresh	938730.0	891793.5	2522.8	2522.8	2500
40/60_WG_Fresh	737920.0	701024.0	3177.7		
40/60_BD_Fresh	761990.0	723890.5	5035.2		
40/60_GR_Fresh	689330.0	654863.5	5036.0		
40/60_QZ_Fresh	709370.0	673901.5	5036.5		
40/60_BE_Fresh	761550.0	723472.5	5035.0		
40/60_WG60K_Aged	2728200.0	2591790.0	7972.2		
40/60_WG_Aged	2249900.0	2137405.0	6334.8		
40/60_BD_Aged	2523500.0	2397325.0	10031.0		
40/60_GR_Aged	2413000.0	2292350.0	10033.0		
40/60_QZ_Aged	2334500.0	2217775.0	10034.0		
40/60_BE_Aged	2684600.0	2550370.0	6330.7		

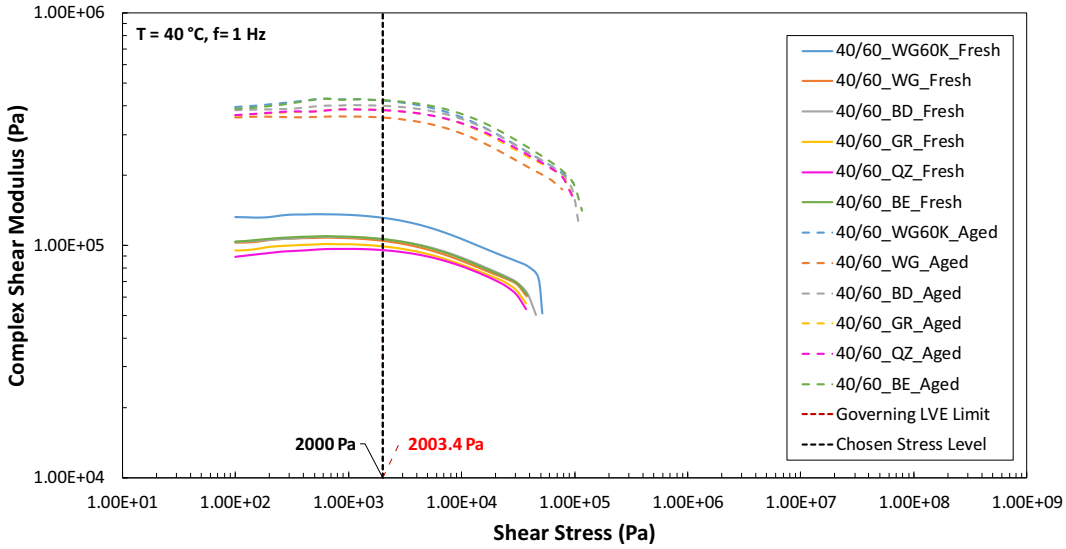

Fig. A6. Mastics amplitude sweep test results. T = 40 °C, f = 1 Hz.

Table A6
Mastics LVE limits. T = 40 °C, f = 1 Hz.

Mastic	G^*_{max} (Pa)	$0.95G^*_{max}$ (Pa)	τ_{limit} (Pa)	$\tau_{governing}$ (Pa)	τ_{chosen} (Pa)
40/60_WG60K_Fresh	136340.0	129523.0	2003.4	2003.4	2000
40/60_WG_Fresh	108190.0	102780.5	2516.6		
40/60_BD_Fresh	109110.0	103654.5	3166.9		
40/60_GR_Fresh	101450.0	96377.5	2517.9		
40/60_QZ_Fresh	96482.0	91657.9	3168.3		
40/60_BE_Fresh	109960.0	104462.0	2517.5		
40/60_WG60K_Aged	428080.0	406676.0	3178.1		
40/60_WG_Aged	360590.0	342560.5	3998.2		
40/60_BD_Aged	401150.0	381092.5	5031.8		
40/60_GR_Aged	385050.0	365797.5	3999.0		
40/60_QZ_Aged	385240.0	365978.0	3999.2		
40/60_BE_Aged	429680.0	408196.0	3999.3		

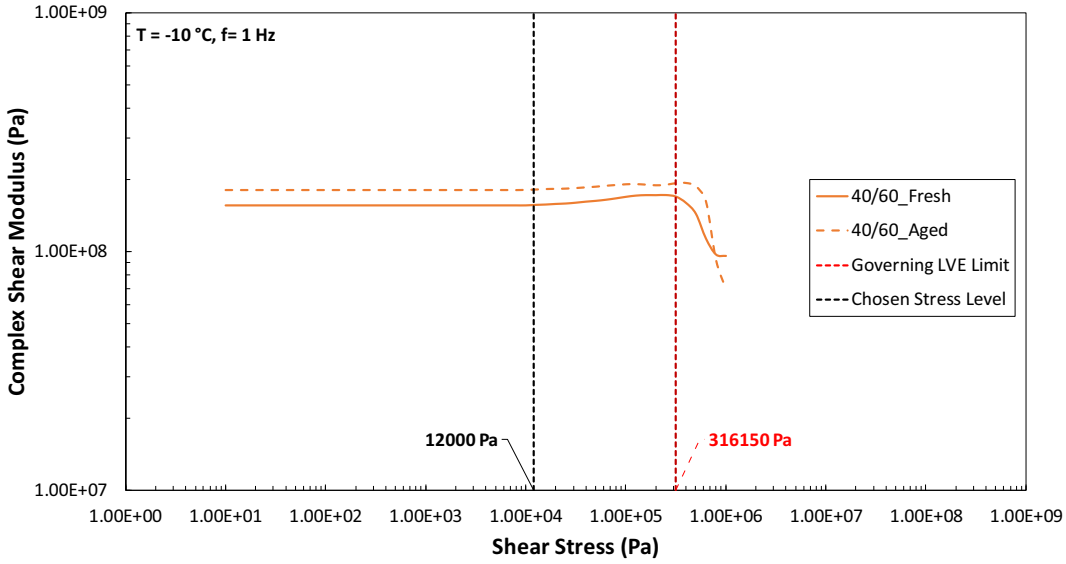

Fig. A7. Bitumen amplitude sweep test results. T = −10 °C, f = 1 Hz.

Table A7
Bitumen LVE limits. T = −10 °C, f = 1 Hz.

Bitumen	G^*_{max} (Pa)	$0.95G^*_{max}$ (Pa)	τ_{limit} (Pa)	$\tau_{governing}$ (Pa)	τ_{chosen} (Pa)
40/60_Fresh	173240000.0	164578000.0	316150.0	316150	12000
40/60_Aged	193430000.0	183758500.0	501060.0		

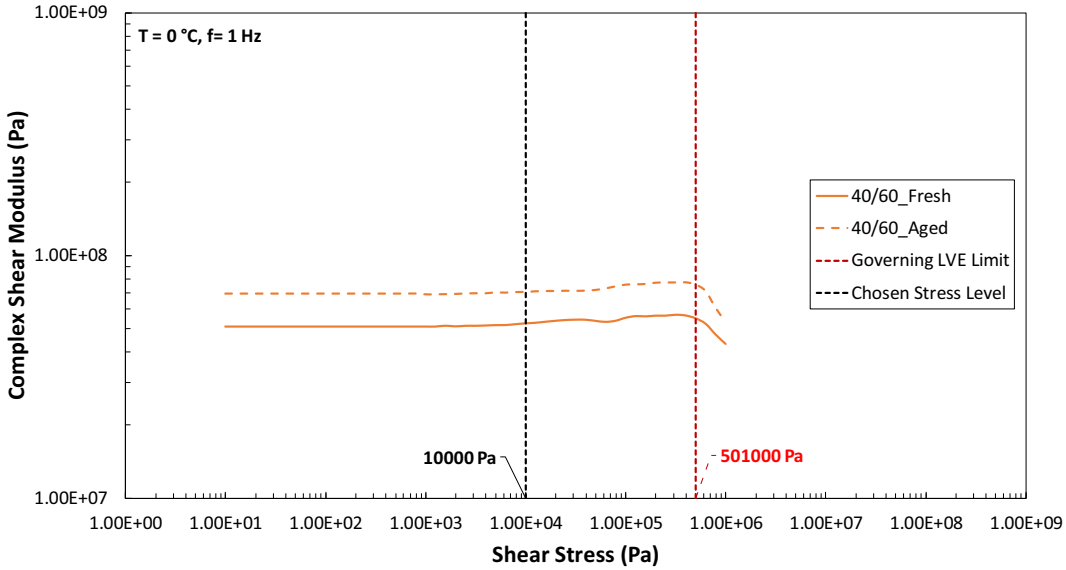

Fig. A8. Bitumen amplitude sweep test results. T = 0 °C, f = 1 Hz.

Table A8
Bitumen LVE limits. T = 0 °C, f = 1 Hz.

Bitumen	G^*_{max} (Pa)	$0.95G^*_{max}$ (Pa)	τ_{limit} (Pa)	$\tau_{governing}$ (Pa)	τ_{chosen} (Pa)
40/60_Fresh	56878000.0	54034100.0	501020.0	501000	10000
40/60_Aged	77643000.0	73760850.0	501000.0		

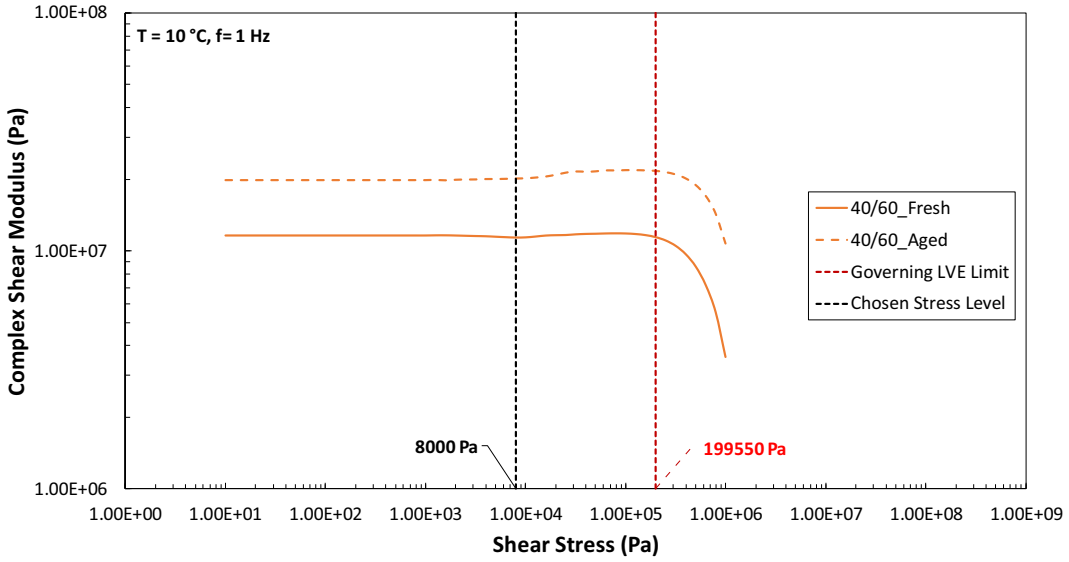

Fig. A9. Bitumen amplitude sweep test results. T = 10 °C, f = 1 Hz.

Table A9
Bitumen LVE limits. T = 10 °C, f = 1 Hz.

Bitumen	G^*_{max} (Pa)	$0.95G^*_{max}$ (Pa)	τ_{limit} (Pa)	$\tau_{governing}$ (Pa)	τ_{chosen} (Pa)
40/60_Fresh	11836000.0	11244200.0	199550.0	199550	8000
40/60_Aged	21868000.0	20774600.0	316060.0		

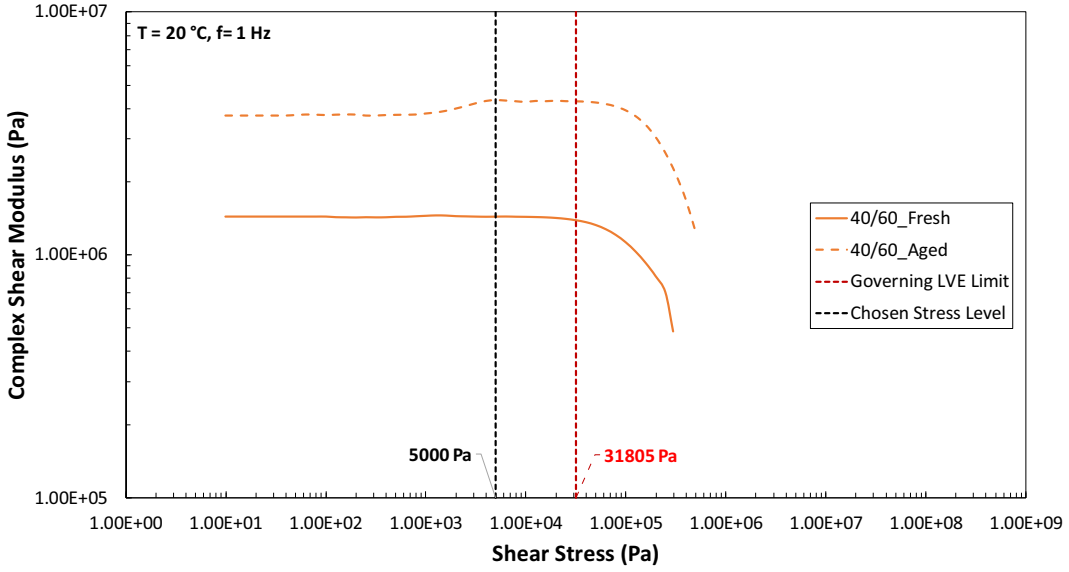

Fig. A10. Bitumen amplitude sweep test results. T = 20 °C, f = 1 Hz.

Table A10
Bitumen LVE limits. T = 20 °C, f = 1 Hz.

Bitumen	G^*_{max} (Pa)	$0.95G^*_{max}$ (Pa)	τ_{limit} (Pa)	$\tau_{governing}$ (Pa)	τ_{chosen} (Pa)
40/60_Fresh	1450900.0	1378355.0	31805.0	31805	5000
40/60_Aged	4337500.0	4120625.0	63121.0		

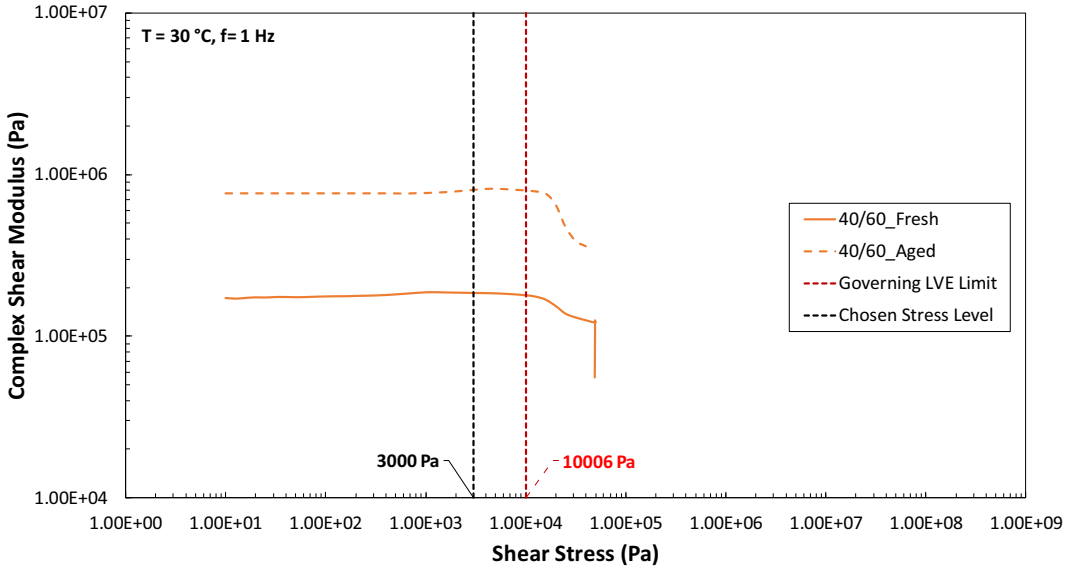

Fig. A11. Bitumen amplitude sweep test results. T = 30 °C, f = 1 Hz.

Table A11
Bitumen LVE limits. T = 30 °C, f = 1 Hz.

Bitumen	G^*_{max} (Pa)	$0.95G^*_{max}$ (Pa)	τ_{limit} (Pa)	$\tau_{governing}$ (Pa)	τ_{chosen} (Pa)
40/60_Fresh	186820.0	177479.0	10006.0	10006	3000
40/60_Aged	815590.0	774810.5	15849.0		

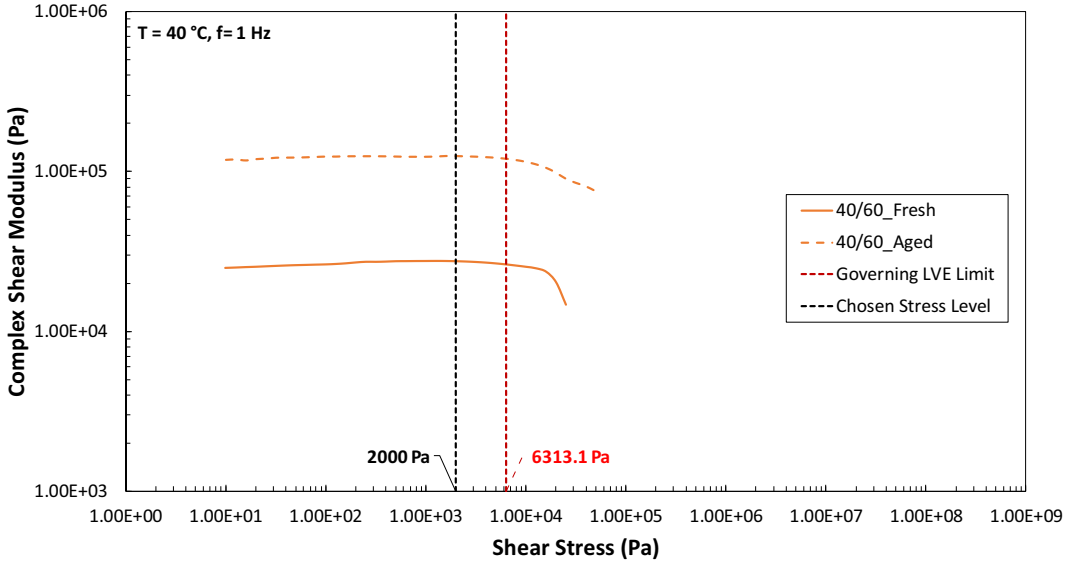

Fig. A12. Bitumen amplitude sweep test results. T = 40 °C, f = 1 Hz.

Table A12
Bitumen LVE limits. T = 40 °C, f = 1 Hz.

Bitumen	G^*_{max} (Pa)	$0.95G^*_{max}$ (Pa)	τ_{limit} (Pa)	$\tau_{governing}$ (Pa)	τ_{chosen} (Pa)
40/60_Fresh	27541.0	26164.0	6333.2	6313.1	2000
40/60_Aged	124940.0	118693.0	6313.1		

Appendix B WLF shift factors, WLF coefficients and modified CAM model fitting parameters

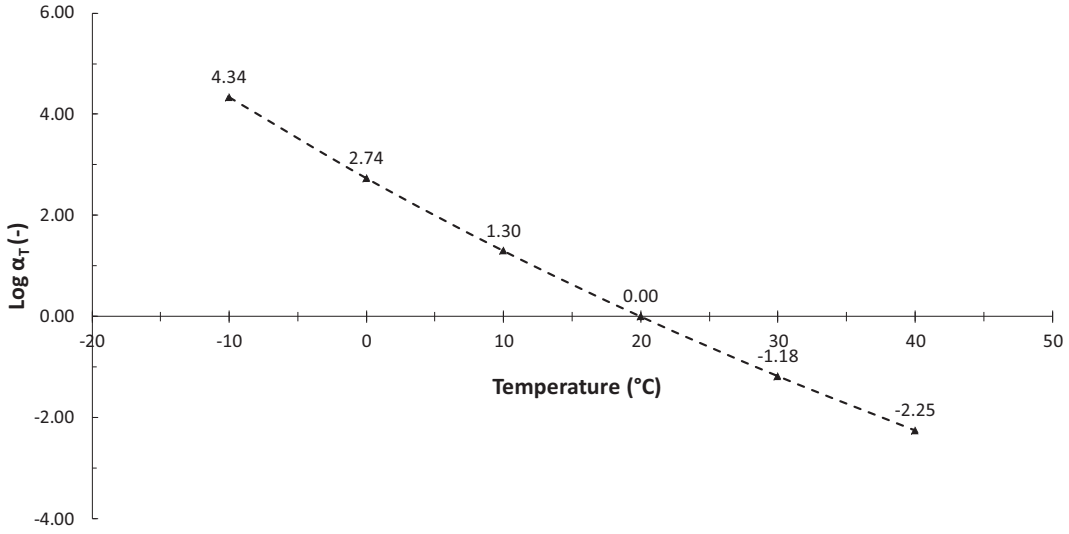

Fig. B1. WLF shift factors. 40/60_WG60K_Fresh.

Table B1
WLF coefficients. 40/60_WG60K_Fresh.

Mastic	WLF Coefficients (−)	
	C_1	C_2
40/60_WG60K_Fresh	25.439	205.834

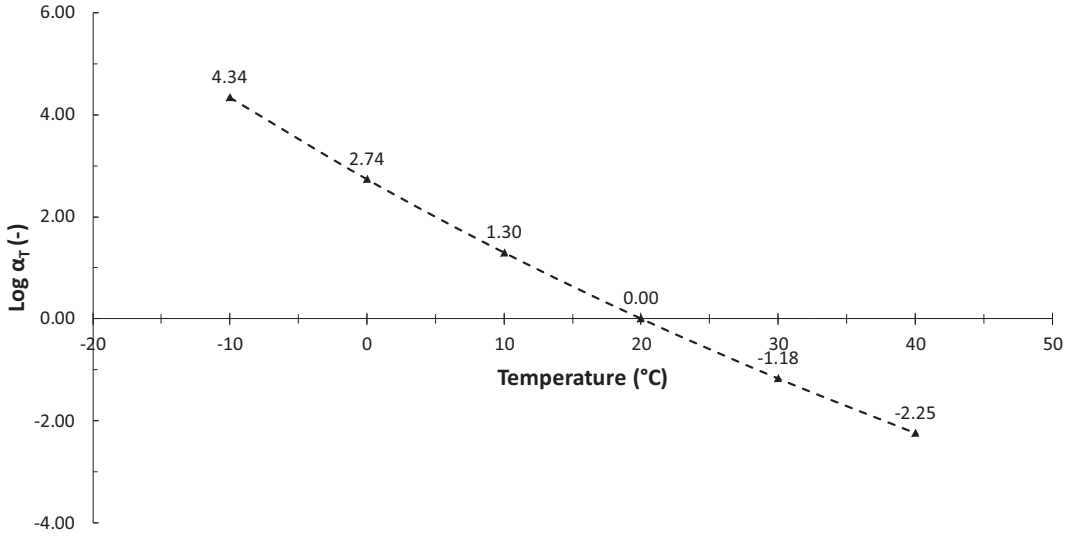

Fig. B2. WLF shift factors. 40/60_WG_Fresh.

Table B2
WLF coefficients. 40/60_WG_Fresh.

Mastic	WLF Coefficients (−)	
	C_1	C_2
40/60_WG_Fresh	25.115	203.652

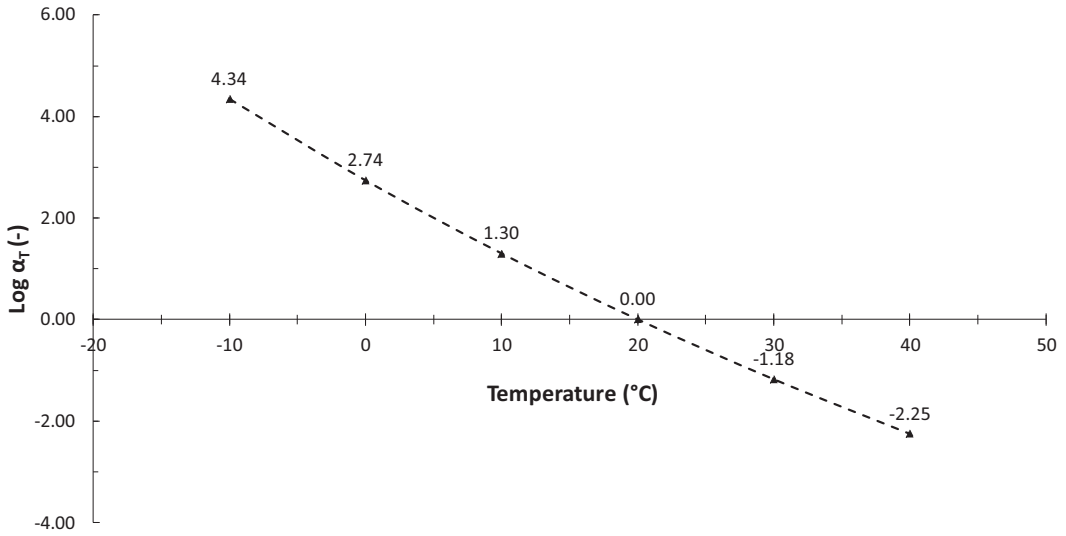

Fig. B3. WLF shift factors. 40/60_BD_Fresh.

Table B3
WLF coefficients. 40/60_BD_Fresh.

Mastic	WLF Coefficients (−)	
	C_1	C_2
40/60_BD_Fresh	25.439	205.834

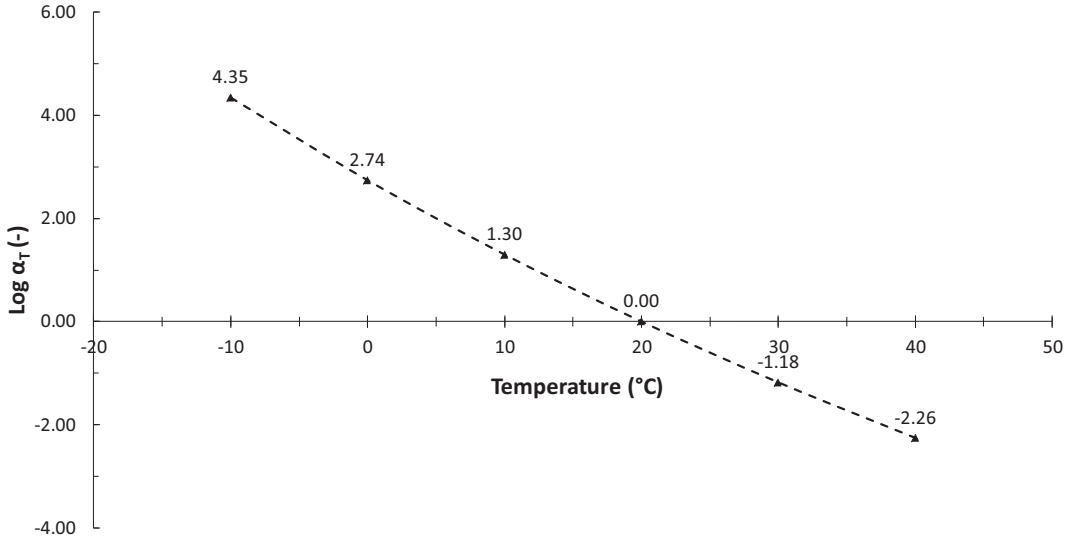

Fig. B4. WLF shift factors. 40/60_GR_Fresh.

Table B4
WLF coefficients. 40/60_GR_Fresh.

Mastic	WLF Coefficients (−)	
	C_1	C_2
40/60_GR_Fresh	25.544	206.369

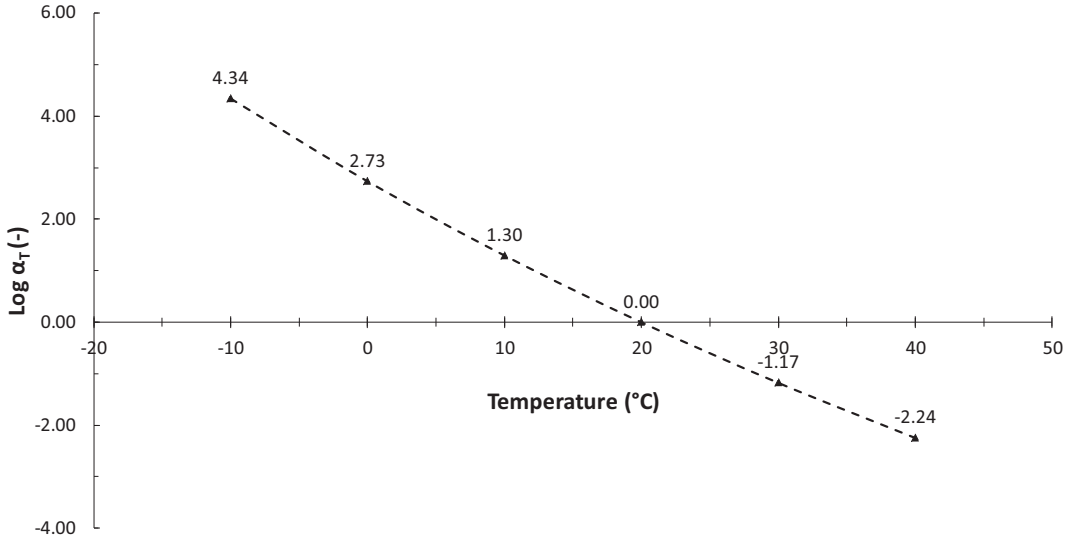

Fig. B5. WLF shift factors. 40/60_QZ_Fresh.

Table B5
WLF coefficients. 40/60_QZ_Fresh.

Mastic	WLF coefficients (−)	
	C_1	C_2
40/60_QZ_Fresh	24.933	202.377

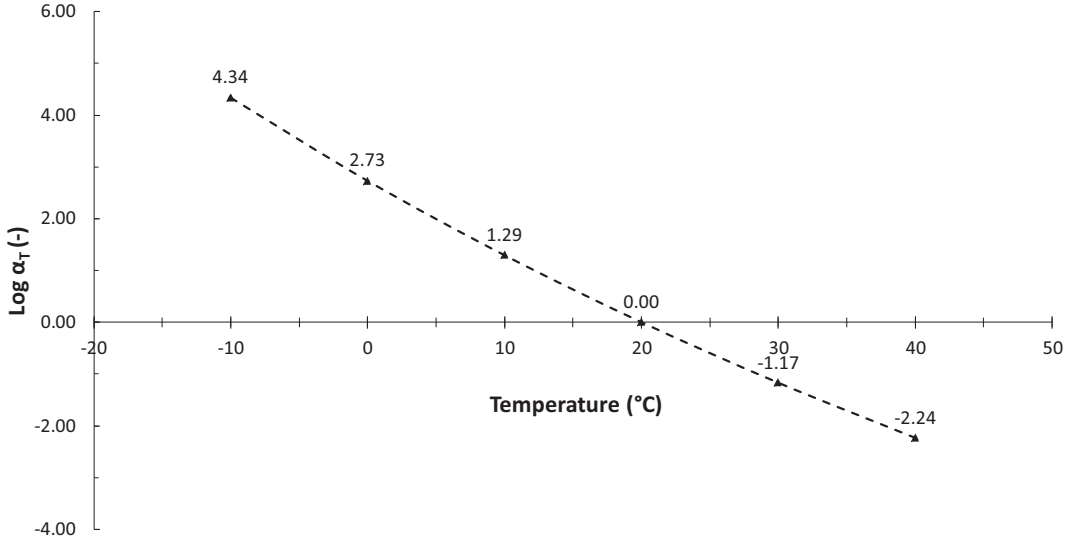

Fig. B6. WLF shift factors. 40/60_BE_Fresh.

Table B6
WLF coefficients. 40/60_QZ_Fresh.

Mastic	WLF Coefficients (−)	
	C_1	C_2
40/60_BE_Fresh	24.653	200.433

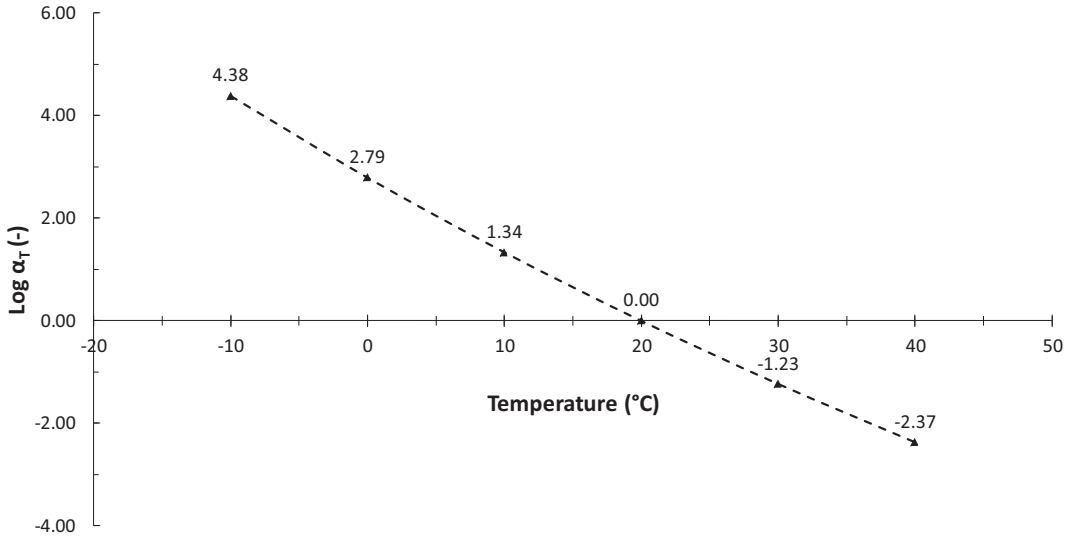

Fig. B7. WLF shift factors. 40/60_WG60K_Aged.

Table B7
WLF coefficients. 40/60_WG60K_Aged.

Mastic	WLF Coefficients (−)	
	C_1	C_2
40/60_WG60K_Aged	31.138	243.173

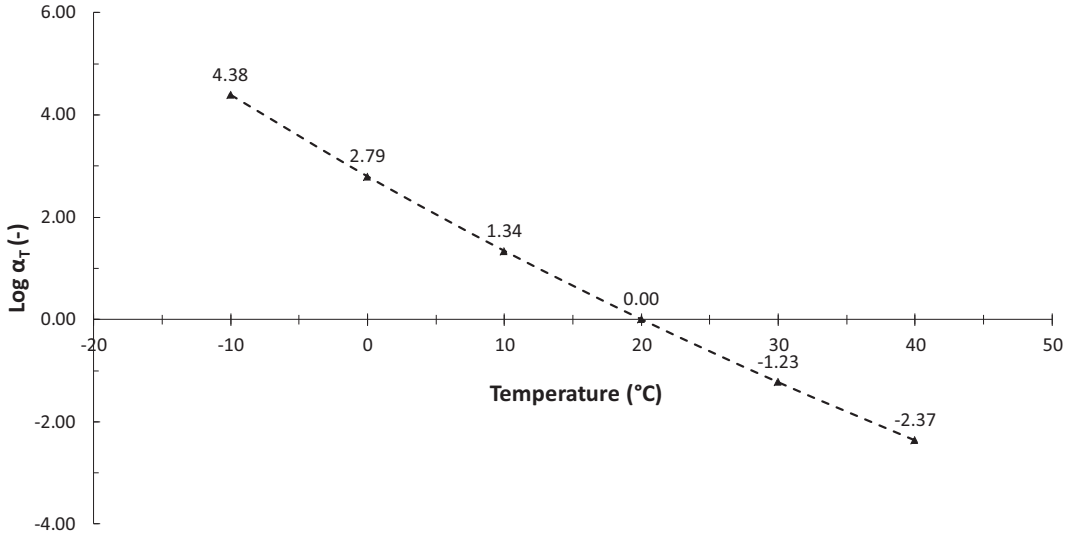

Fig. B8. WLF shift factors. 40/60_WG_Aged.

Table B8
WLF coefficients. 40/60_WG_Aged.

Mastic	WLF Coefficients (−)	
	C_1	C_2
40/60_WG_Aged	31.138	243.173

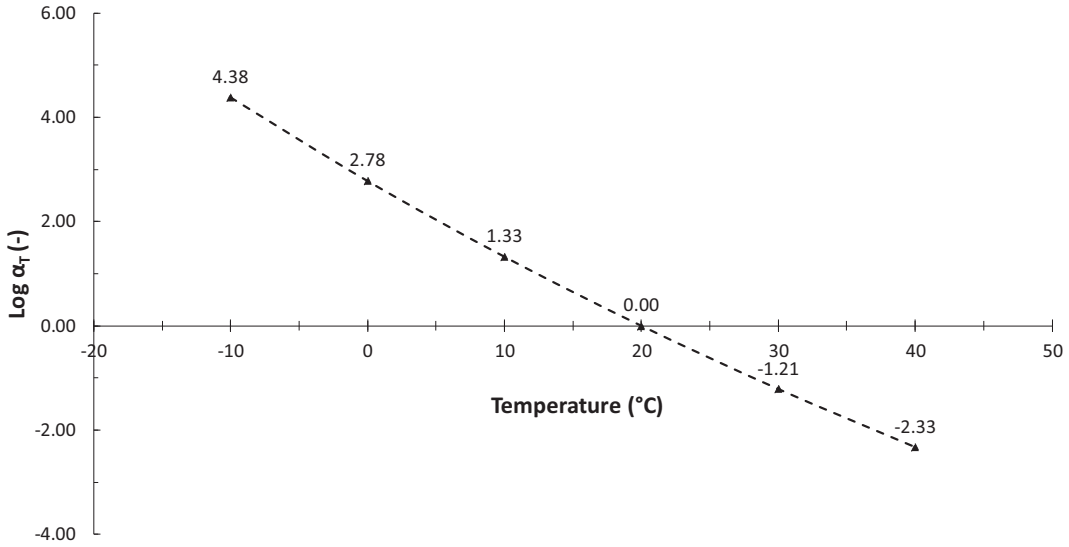

Fig. B9. WLF shift factors. 40/60_BD_Aged.

Table B9
WLF coefficients. 40/60_BD_Aged.

Mastic	WLF Coefficients (−)	
	C_1	C_2
40/60_BD_Aged	28.655	226.161

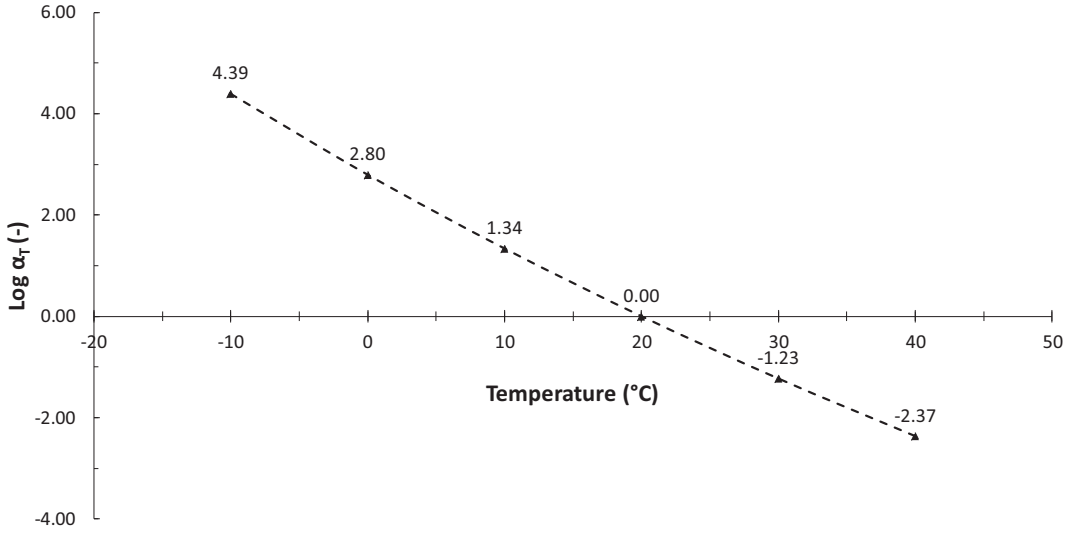

Fig. B10. WLF shift factors. 40/60_GR_Aged.

Table B10
WLF coefficients. 40/60_GR_Aged.

Mastic	WLF Coefficients (−)	
	C_1	C_2
40/60_GR_Aged	31.003	241.828

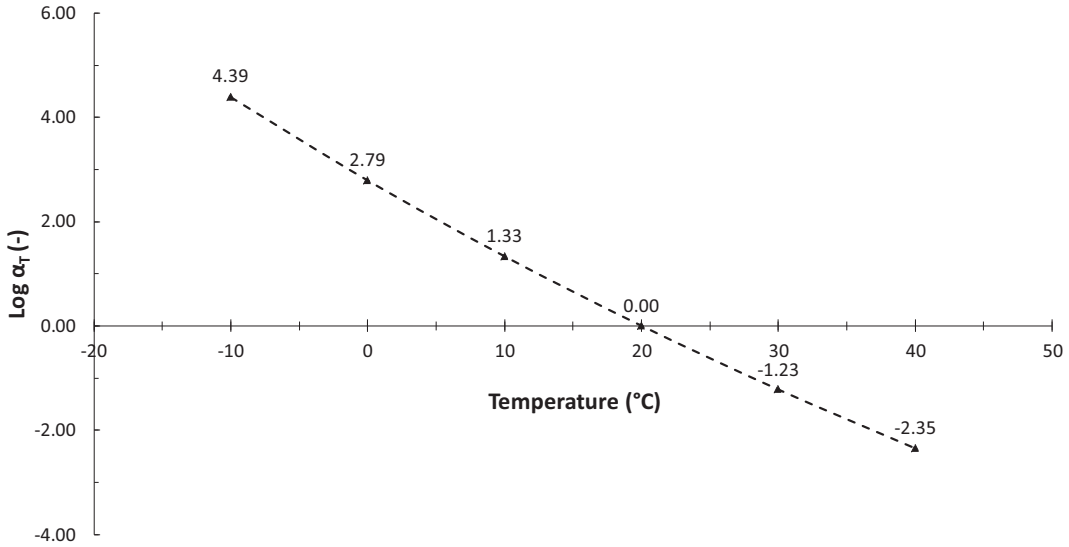

Fig. B11. WLF shift factors. 40/60_QZ_Aged.

Table B11
WLF coefficients. 40/60_QZ_Aged.

Mastic	WLF Coefficients (−)	
	C_1	C_2
40/60_QZ_Aged	30.154	236.123

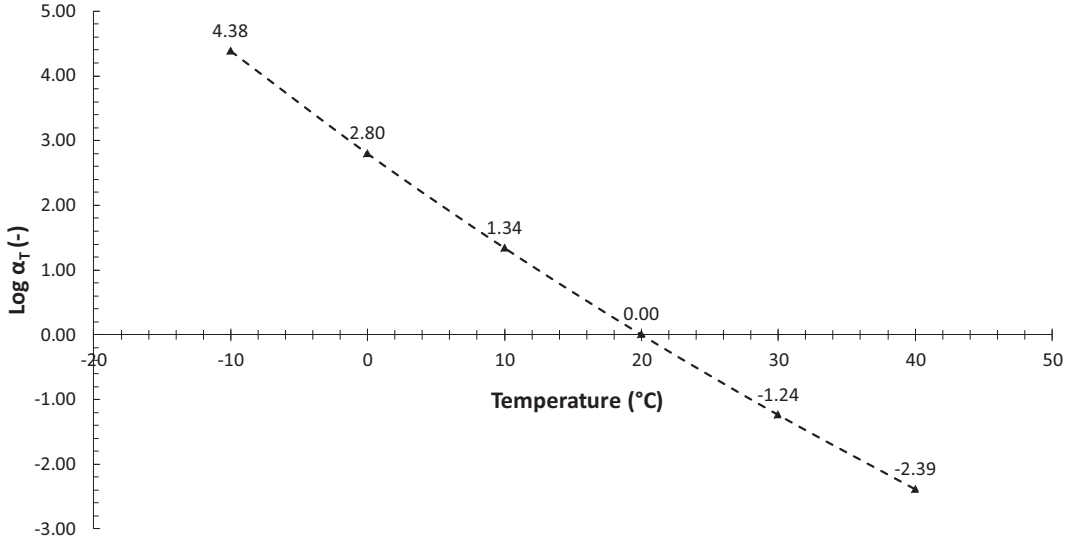

Fig. B12. WLF shift factors. 40/60_BE_Aged.

Table B12
WLF coefficients. 40/60_BE_Aged.

Mastic	WLF Coefficients (−)	
	C_1	C_2
40/60_BE_Aged	32.529	252.767

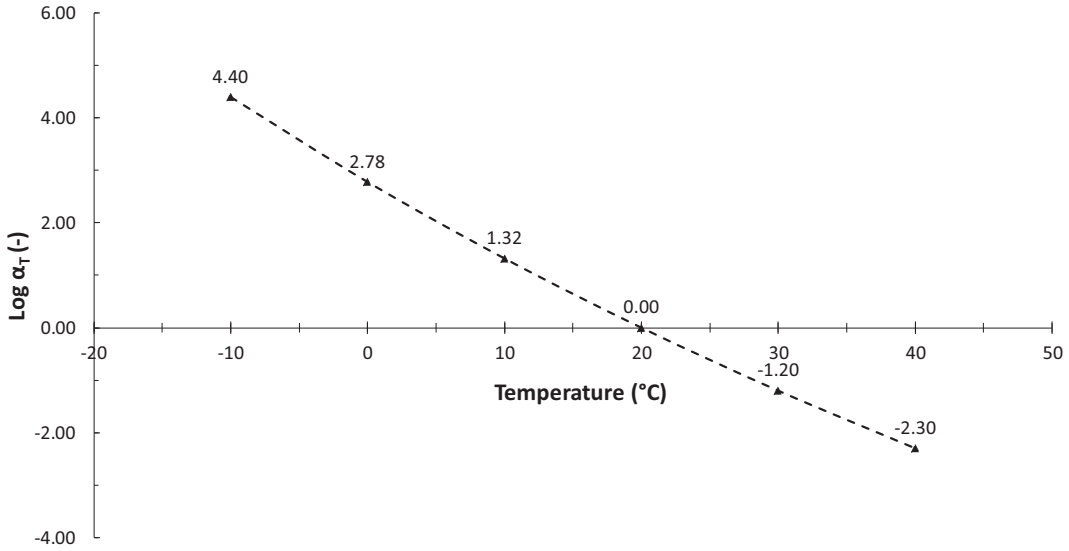

Fig. B13. WLF shift factors. 40/60_Fresh.

Table B13
WLF coefficients. 40/60_Fresh.

Bitumen	WLF Coefficients (−)	
	C_1	C_2
40/60_Fresh	26.594	211.485

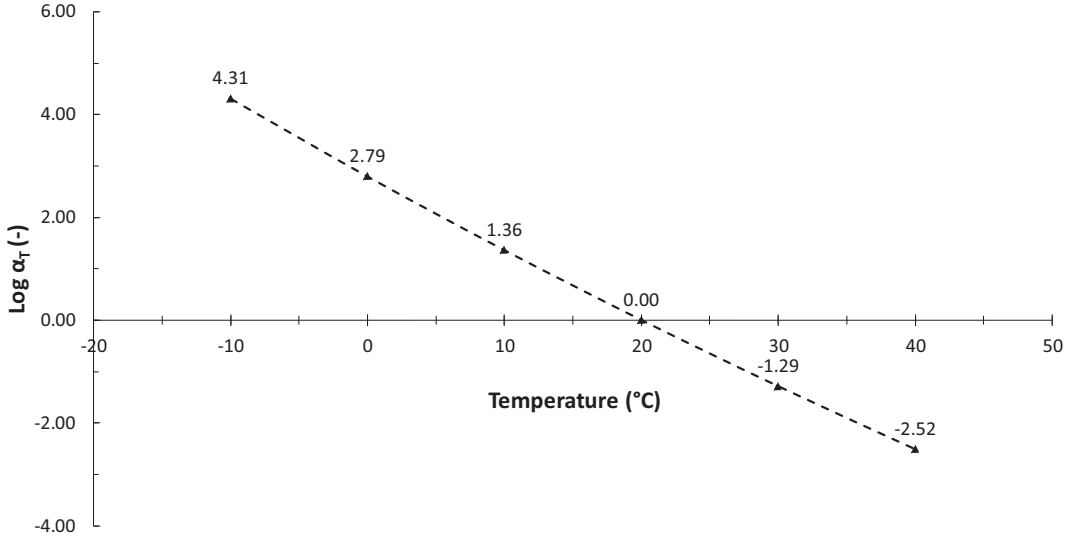

Fig. B14. WLF shift factors. 40/60_Aged.

Table B14
WLF coefficients. 40/60_Aged.

Bitumen	WLF Coefficients (−)	
	C_1	C_2
40/60_Aged	50.627	382.405

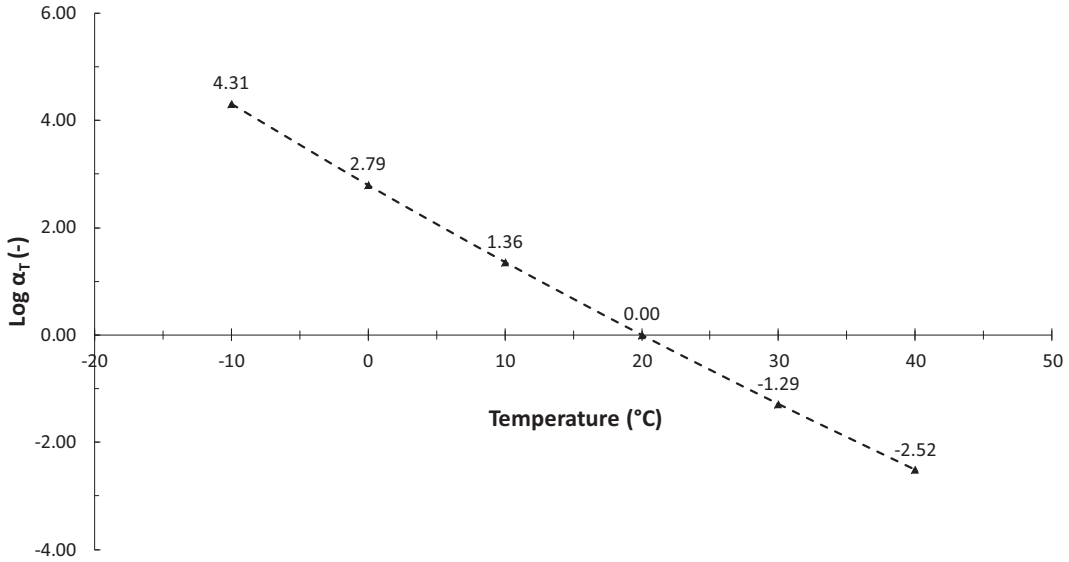

Fig. B15. WLF shift factors. RB_40/60_WG60K_Aged.

Table B15
WLF shift factors. RB_40/60_WG60K_Aged.

Bitumen	WLF Coefficients (−)	
	C_1	C_2
RB_40/60_WG60K_Aged	50.627	382.405

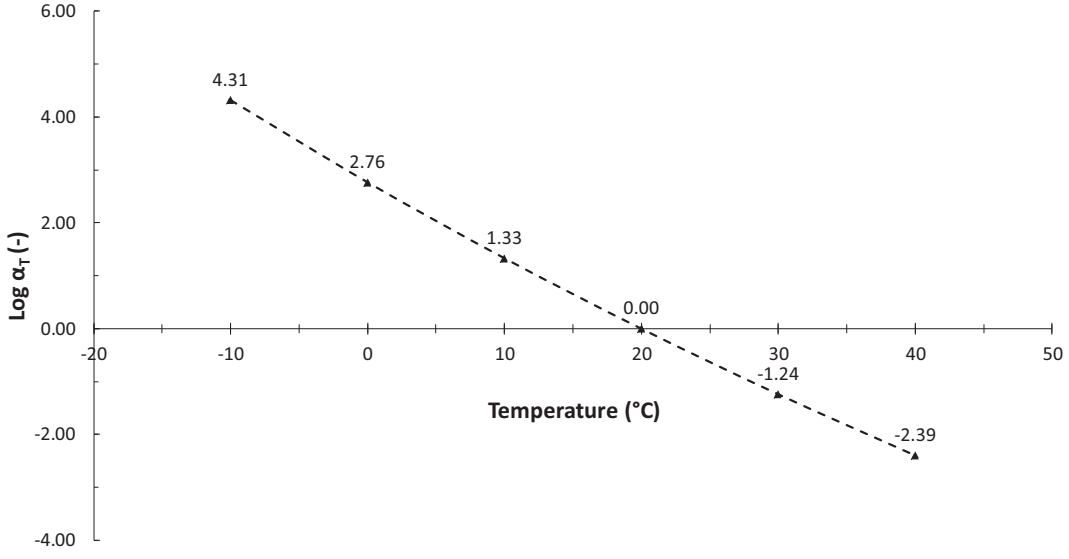

Fig. B16. WLF shift factors. RB_40/60_WG_Aged.

Table B16
WLF shift factors. RB_40/60_WG_Aged.

Bitumen	WLF Coefficients (−)	
	C_1	C_2
RB_40/60_WG_Aged	35.582	277.446

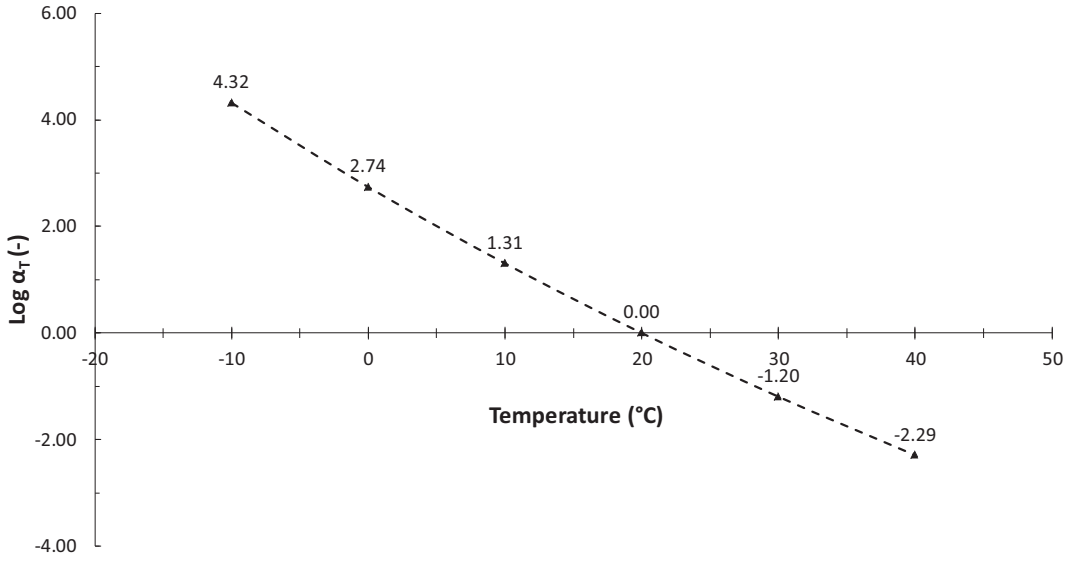

Fig. B17. WLF shift factors. RB_40/60_BD_Aged.

Table B17
WLF shift factors. RB_40/60_BD_Aged.

Bitumen	WLF Coefficients (−)	
	C_1	C_2
RB_40/60_BD_Aged	28.177	225.701

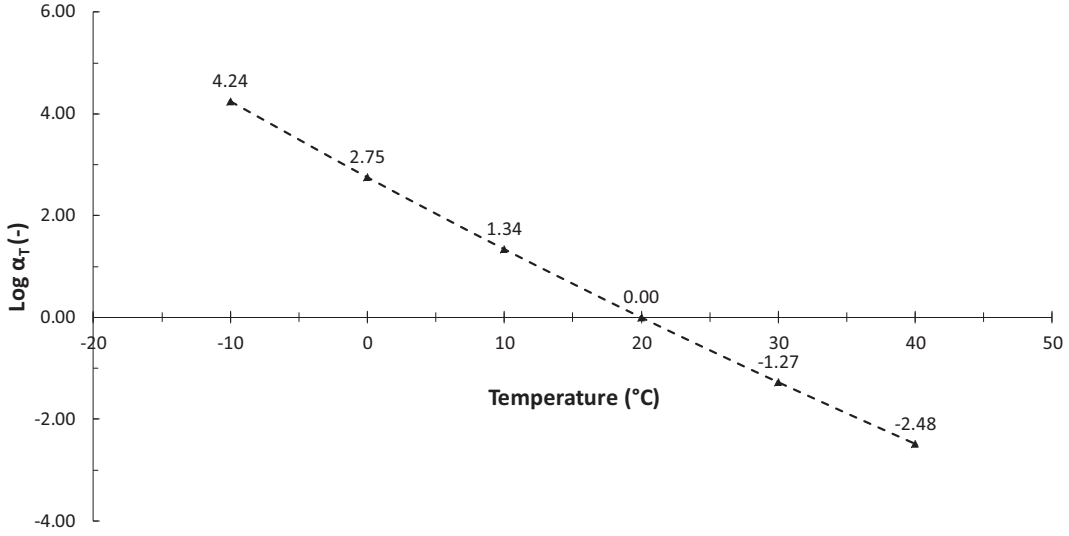

Fig. B18. WLF shift factors. RB_40/60_GR_Aged.

Table B18
WLF shift factors. RB_40/60_GR_Aged.

Bitumen	WLF Coefficients (−)	
	C_1	C_2
RB_40/60_GR_Aged	50.616	387.799

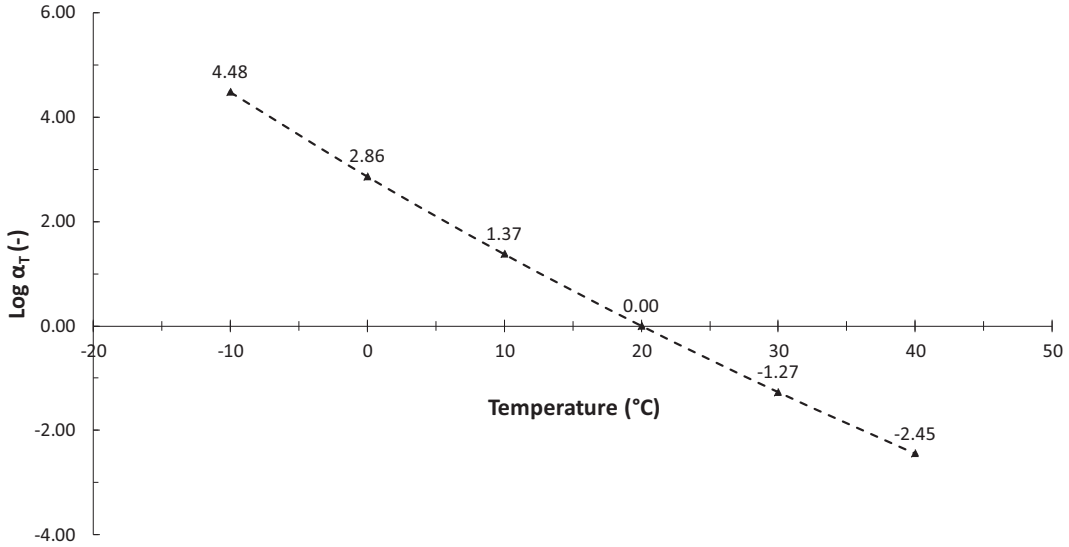

Fig. B19. WLF shift factors. RB_40/60_QZ_Aged.

Table B19
WLF shift factors. RB_40/60_QZ_Aged.

Bitumen	WLF Coefficients (−)	
	C_1	C_2
RB_40/60_QZ_Aged	34.287	259.481

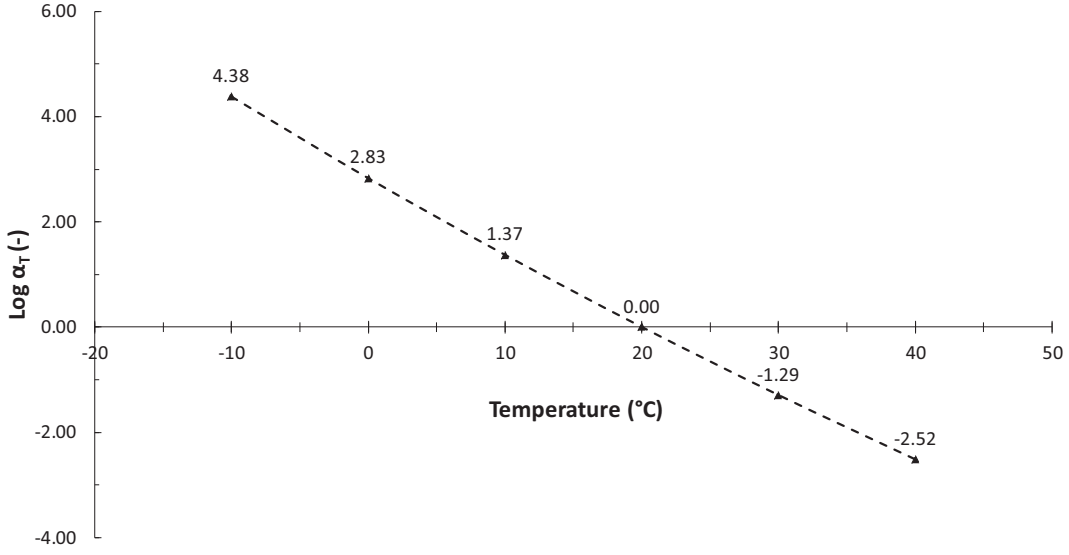

Fig. B20. WLF shift factors. RB_40/60_BE_Aged.

Table B20
WLF shift factors. RB_40/60_BE_Aged.

Bitumen	WLF Coefficients (−)	
	C_1	C_2
RB_40/60_BE_Aged	45.620	342.280

Table B21
Modified CAM model fitting parameters.

Material	G^*_e (GPa)	G^*_g (GPa)	f_c (Hz)	δ_e (°)	δ_g (°)	f_d (Hz)	k (−)	m (−)
40/60_WG60K_Fresh	0	2.32	3.500	86.50	0	7.5E−05	0.175	1.22
40/60_WG_Fresh	0	2.04	3.344	87.50	0	5.4E−05	0.173	1.22
40/60_BD_Fresh	0	2.01	2.737	88.00	0	3.1E−05	0.169	1.23
40/60_GR_Fresh	0	2.85	2.855	89.00	0	9.6E−06	0.160	1.25
40/60_QZ_Fresh	0	2.76	3.294	89.00	0	1.1E−05	0.160	1.24
40/60_BE_Fresh	0	2.22	2.622	88.00	0	2.2E−05	0.166	1.25
40/60_WG60K_Aged	0	2.23	0.158	87.50	0	4.5E−07	0.154	1.31
40/60_WG_Aged	0	2.00	0.162	87.50	0	2.9E−07	0.149	1.29
40/60_BD_Aged	0	2.25	0.078	87.50	0	5.5E−08	0.143	1.34
40/60_GR_Aged	0	234	0.082	87.50	0	4.9E−08	0.142	1.33
40/60_QZ_Aged	0	2.21	0.116	87.50	0	8.4E−08	0.143	1.30
40/60_BE_Aged	0	2.24	0.100	87.50	0	8.4E−08	0.144	1.31
40/60_Fresh	0	1.51	3.470	90.00	0	2.5E−06	0.147	1.26
40/60_Aged	0	1.61	0.211	89.00	0	3.8E−09	0.126	1.21
RB_40/60_WG60K_ Aged	0	1.67	0.119	90.00	0	1.1E−09	0.122	1.26
RB_40/60_WG_Aged	0	1.49	0.056	90.00	0	7.6E−10	0.123	1.34
RB_40/60_BD_Aged	0	1.70	0.089	89.00	0	8.6E−10	0.122	1.30
RB_40/60_GR_Aged	0	1.67	0.203	90.00	0	2.9E−09	0.125	1.24
RB_40/60_QZ_Aged	0	1.79	0.024	90.00	0	6.1E−11	0.115	1.33
RB_40/60_BE_Aged	0	1.73	0.094	89.00	0	6.2E−10	0.120	1.25

References

[1] R. Moraes, H.U. Bahia, Effect of mineral fillers on the oxidative aging of asphalt binders: Laboratory study with mastics, Transport. Res. Rec. J. Transport. Res. Board 2506 (2015) 19–31.

[2] D.A. Anderson, H.U. Bahia, R. Dongre, Rheological properties of mineral filler-asphalt mastics and their relationship to pavement performance, effects of aggregates and mineral fillers on asphalt mixture performance, American Society for Testing Materials, Philadelphia, Pa, 1992.

[3] R.M. Alfaqawi, G.D. Airey, D. Lo Presti, J. Grenfell, Effects of Mineral Fillers on Bitumen Mastic Chemistry and Rheology, University of Nottingham, 2017.

[4] R. Han, Improvement to a transport model of asphalt binder oxidation in pavements: Pavement temperature modeling, oxygen diffusivity in asphalt binders and mastics and pavement air void characterization, Texas A&M University, College Station, TX, Ph.D. Thesis, 2011.

[5] J.G. Charles, A. Epps Martin, A. Chowdhury, R. Han, N. Prapaitrakul, X. Jin & J. Lawrence, Evaluation of binder aging and its influence in aging of hot mix asphalt concrete: Literature review and experimental design, Federal Highway Administration (FHWA): Report No. FHWA/TX-08/0-6009-1, Report 0-6009-1, Austin, Texas, 2009.

[6] J.C. Petersen, F.A. Barbour, S.M. Dorrence, Catalysis of asphalt oxidation by mineral aggregate surface and asphalt components, Proc. Assoc. Asphalt Pav. Technol. 43 (1974) 162–177.

[7] J. Wu, The influence of mineral aggregates and binder volumetrics on bitumen ageing, University of Nottingham, Ph.D. Thesis, 2009.

[8] C.W. Curtis, K. Emsley & J. Epps, Fundamental properties of asphalt aggregate interactions including adhesion and absorption, Strategic Highway research Program: Report No. SHRP-A-341, National Research Council, Washington D.C., 1993.

[9] R. Gubler, Y. Liu, D.A. Anderson, M.N. Partl, Investigation of the system filler and asphalt binders by rheological means, Assoc. Asphalt Pav. Technol. (AAPT) 68 (1999) 284–304.

[10] R. Moraes, H.U. Bahia, Effect of mineral filler on changes in molecular size distribution of asphalts during oxidative ageing, Road Mater. Pavement Design 16 (sup2) (2015) 55–72.

[11] A. Gundla, J. Medina, P. Gudipudi, R. Stevens, R. Salim, W. Zeiada, B. Shane Underwood, Investigation of aging in hydrated lime and Portland cement modified asphalt concrete at multiple length scales, J. Mater. Civ. Eng. 28 (5) (2016) 04015205, https://doi.org/10.1061/(ASCE)MT.1943-5533.0001501.

[12] J.C. Petersen, H. Plancher & P.M. Harnsberger, Lime treatment of asphalt to reduce age hardening and improve flow properties, Proceedings of the Association Asphalt Paving Technologists, Lino Lakers, MN: Association Asphalt Paving Technologists (AAPT), 56, 632–653, 1987.

[13] D. Lesueur, J. Petit, H.-J. Ritter, The mechanisms of hydrated lime modification of asphalt mixtures: a state-of-the-art review, Road Mater. pavement Design 14 (1) (2013) 1–16.

[14] A. Varveri, Moisture damage susceptibility of asphalt mixtures, experimental characterization and modelling, Delft University of Technology, Ph.D. Thesis, 2017.

[15] National Cooperative Highway Research Program (NCHRP), Test methods and specification criteria for mineral filler used in HMA, Project 9-45, University of Wisconsin-Madison,2010.

[16] K. Schellenberg, H.J. Eulitz, Verbesserung von asphalteigenschapen durch einsatz von kalkhydrat, Bitumen 1 (1999) 2–8.

[17] W. Grobowski, J. Wilanowicz & T. Sobol, Structural and functional properties of mineral fillers modified with hydrated lime, Proceedings 6th International Conference on Maintenance and Rehabilitation of Pavements and Technological Control (MAIERPAV6), Torino (Italy), Paper 78, 2009.

[18] P.D.C. Nageswaran, Adhesion of aggregate-binder systems, Delft University of Technology, M.Sc. Thesis, 2016.

[19] G.D. Airey, State of the art report on ageing test methods for bituminous pavement materials, Int. J. Pavement Eng. 4 (3) (2003) 165–176.

[20] D. Lesueur, A. Teixeira, M.M. Lázaro, D. Andaluz, A. Ruiz, A simple test method in order to assess the effect of mineral fillers on bitumen ageing, Constr. Build. Mater. 117 (2016) 182–189.

[21] J.C. Petersen, R.E. Robertson, J.F. Branthaver, P.M. Harnsberger, J.J. Duvall, S.S. Kim, D.A. Anderson, D.W. Christiansen, H.U. Bahia, R. Dongre, M.G. Sharma, C.E. Antle, J.W. Button & C.J. Glover, Binder characterization and evaluation, vol. 4, Strategic Highway Research Program: Report No. SHRP-A-370, Washington, D. C., 1994.

[22] N.I.M. Yusoff, M.T. Shaw, G.D. Airey, Modelling the linear viscoelastic rheological properties of bituminous binders, Constr. Build. Mater. 25 (5) (2011) 2171–2189.

[23] B. Hofko, M.Z. Alavi, H. Grothe, D. Jones, J. Harvey, Repeatability and sensitivity of FTIR ATR spectral analysis methods for bituminous binders, Mater. Struct. 50 (187) (2017) 1–15.

[24] D.A. Anderson & R. Bonaquist. Investigation of short-term laboratory ageing of neat and modified asphalt binders, NCHRP Report 709, National Cooperative Highway Research Program, Transportation Research Board of the National Academies, Washington D.C., 2012.